

Columns with End Restraint and Bending in Load and Resistance Design Factor

W. F. CHEN and E. M. LUI

1. INTRODUCTION

Elastic Stability—Mathematical

The problem of structural stability has long been the subject of research for a number of researchers. Early in the 18th century, Euler¹ investigated the elastic stability of a centrally loaded isolated strut using the bifurcation approach. The bifurcation or eigenvalue approach is basically a mathematical approach. Under the assumptions that (1) the member is perfectly straight, (2) the material remains fully elastic and obeys Hooke's Law and (3) the deflection is small, a linear differential equation can be written based on a slightly deformed geometry of the member.

The eigenvalue solution to the characteristic equation of this differential equation will give the buckling load of the strut. This load corresponds to the state at which bifurcation of equilibrium takes place. At this load, the original straight position of the member ceases to be stable. Under this load, a small lateral disturbance will produce a large lateral displacement which will not disappear when the disturbance is removed. This buckling load is referred to as the critical load or Euler load given by

$$P_e = \frac{\pi^2 EI}{(KL)^2} \quad (1)$$

where

- I = moment of inertia of the cross section
- L = unbraced length of the column
- K = effective length factor to account for the end conditions of the column

W. F. Chen is Professor and Head, Structural Engineering Department, School of Engineering, Purdue University, West Lafayette, Indiana.

E. M. Lui is a Graduate Assistant in that same department.

This paper, the T. R. Higgins Lectureship Award winner for 1985, was first presented at the Structural Stability Research Council Annual Technical Session and Meeting on April 16, 1985 in Cleveland, Ohio.

This formula gives a good prediction of the behavior of long columns so far as the axial stresses in the member remain below the proportional limit, i.e., if the member remains fully elastic. For short or intermediate columns, the assumption of fully elastic behavior will be questionable. Under the action of the applied force, some fibers of the cross section will yield. Consequently, only the elastic core of the cross section will be effective in resisting the additional applied force. Thus, the Euler load will overestimate the strength of the column.

Plastic Buckling—Physical

To account for the effect of inelasticity, two theories were proposed:^{2,3} the double modulus theory and the tangent modulus theory. In the double modulus theory (also known as the reduced modulus theory), the axial load is assumed constant during buckling. Consequently, at buckling, the bending deformation of the column will produce strain reversal on the convex side of the member with the result that the elastic modulus E will govern the stress-strain behavior of the fibers. The concave side of the column, on the other hand, will continue to load and so the tangent modulus E_r will govern the stress-strain behavior of the fibers (Fig. 1). The critical load obtained based on this concept is referred to as the reduced modulus load given by

$$P_r = \frac{\pi^2 E_r I}{(KL)^2} = \frac{E_r}{E} P_e \quad (2)$$

where E_r is the reduced modulus.

The reduced modulus is a function of the tangent modulus and the geometry of the cross section. Hence the reduced modulus load depends on both the material property and the geometry of the cross section. The reduced modulus load is lower than the Euler load because the ratio E_r/E in Eq. 2 is always less than unity. It should be pointed out that the reduced modulus load can only be reached if the column is artificially held in a straight position when the tangent modulus load (to be discussed later) has been exceeded. The reduced modulus load can

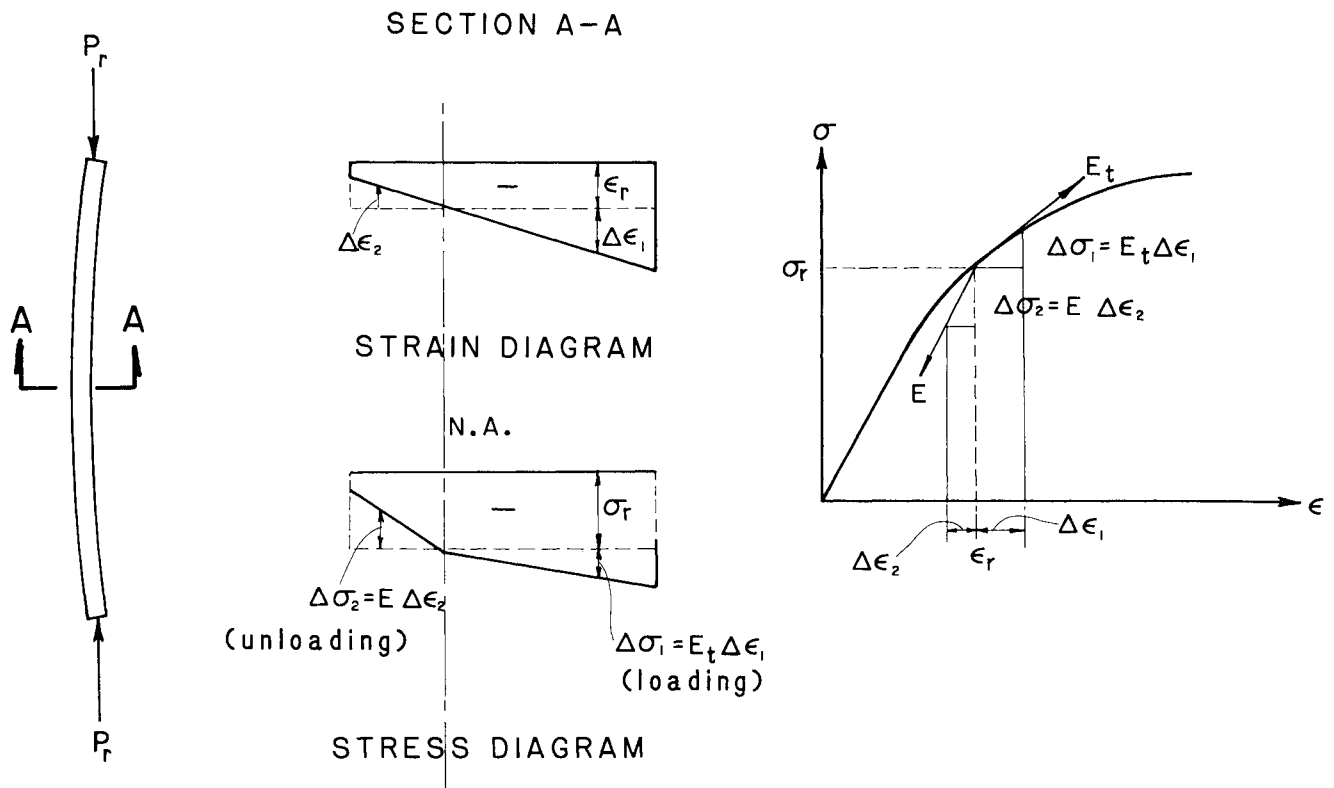


Fig. 1. Double (reduced) modulus theory

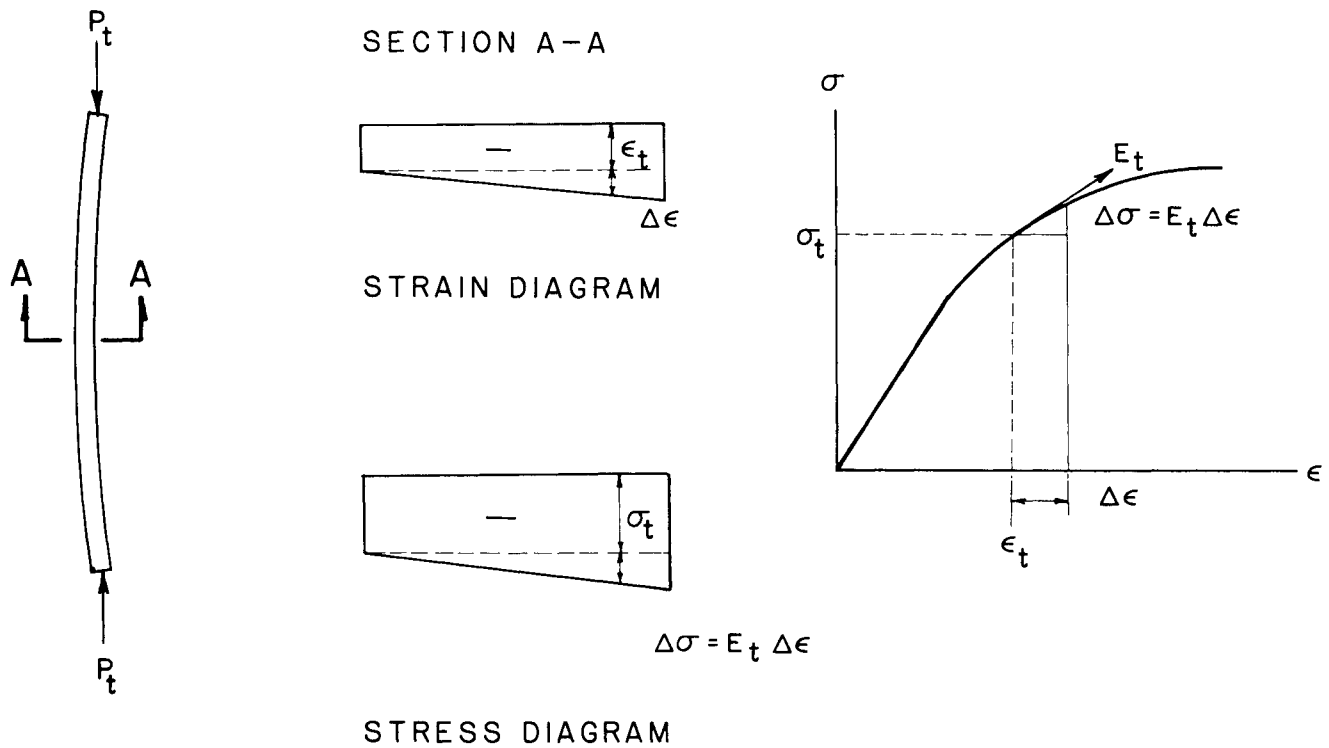


Fig. 2. Tangent modulus theory

never be reached even if the slightest geometrical imperfection is present in the column.

In the tangent modulus theory, the axial load is assumed to increase during buckling. The amount of increase is such that strain reversal will not take place and so the tangent modulus E_t will govern the stress-strain behavior of the entire cross section (Fig. 2). The critical load obtained is known as the tangent modulus load given by

$$P_t = \frac{\pi^2 E_t I}{(KL)^2} = \frac{E_t}{E} P_e \quad (3)$$

The tangent modulus load, unlike the reduced modulus load, is independent of the geometry of the cross section. It depends only on the material property. For a steel column, the nonlinearity of the average stress-strain behavior of the cross-section is due to the presence of residual stress. Residual stresses arise as a result of the manufacturing process. When a compressive axial force is applied to a stub column (very short column), the fi-

bers that have compressive residual stresses will yield first. The fibers that have tensile residual stresses will yield later. As a result, yielding over the cross section of the column is a gradual process, as shown in Fig. 3.

The slope of the stub column stress-strain curve is the tangent modulus E_t of the member. Also shown in the figure is the stress-strain behavior of a coupon. A coupon, unlike a stub column, is free of residual stress. Therefore, its stress-strain relationship exhibits an elastic-perfectly plastic behavior.

The tangent modulus load marks the point of bifurcation of a perfectly straight inelastic column. The tangent modulus load is lower than the Euler and the reduced modulus loads and so it also represents the lowest load at which bifurcation of equilibrium can take place (Fig. 4).

Experiments on columns have demonstrated the failure loads of columns fall nearer to the tangent modulus loads than the reduced modulus loads. The theoretical justification for this observation was given by Shanley,⁴ who, in 1947, investigated the buckling behavior of col-

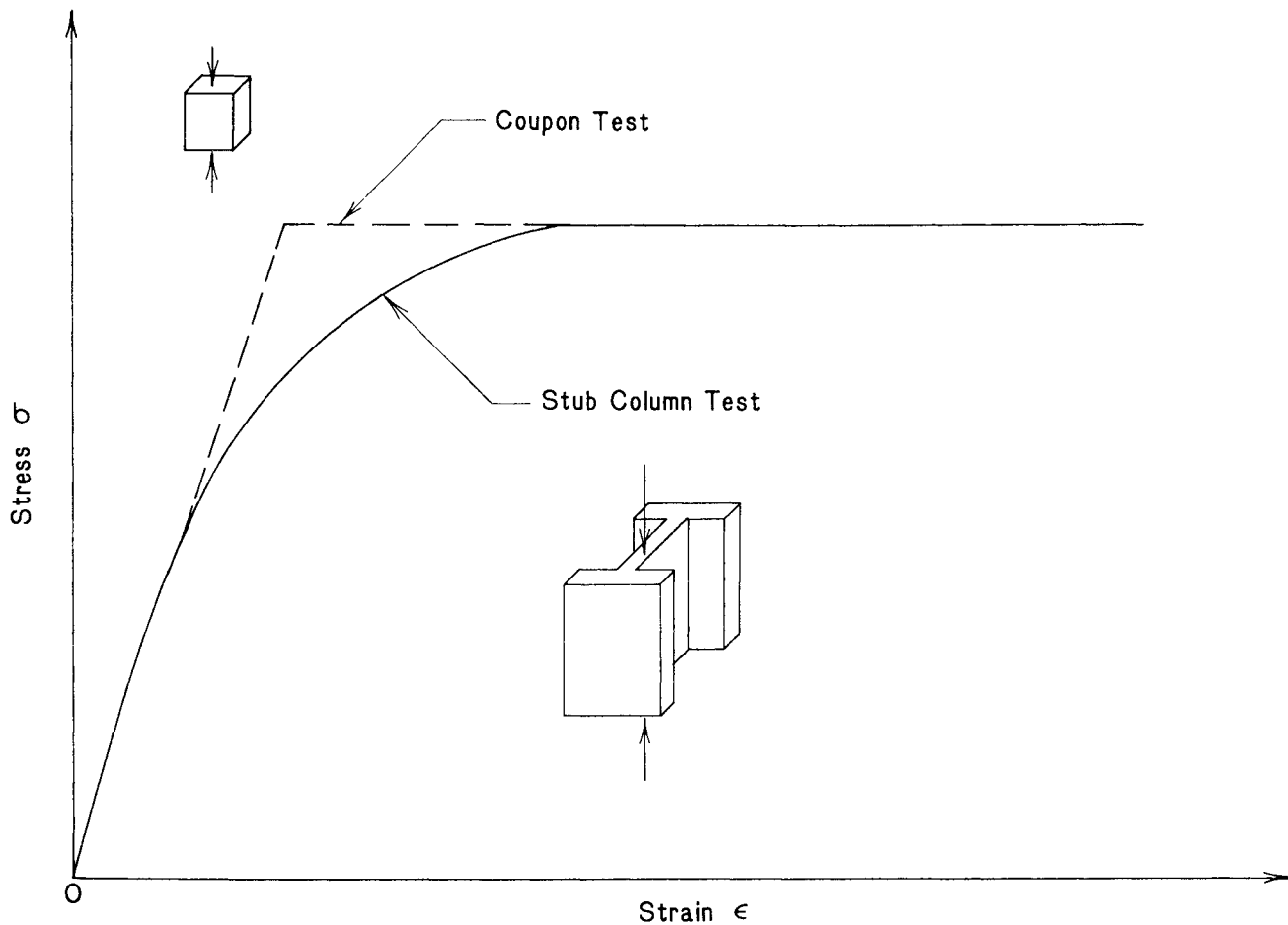


Fig. 3. Stress-strain relationship for steel

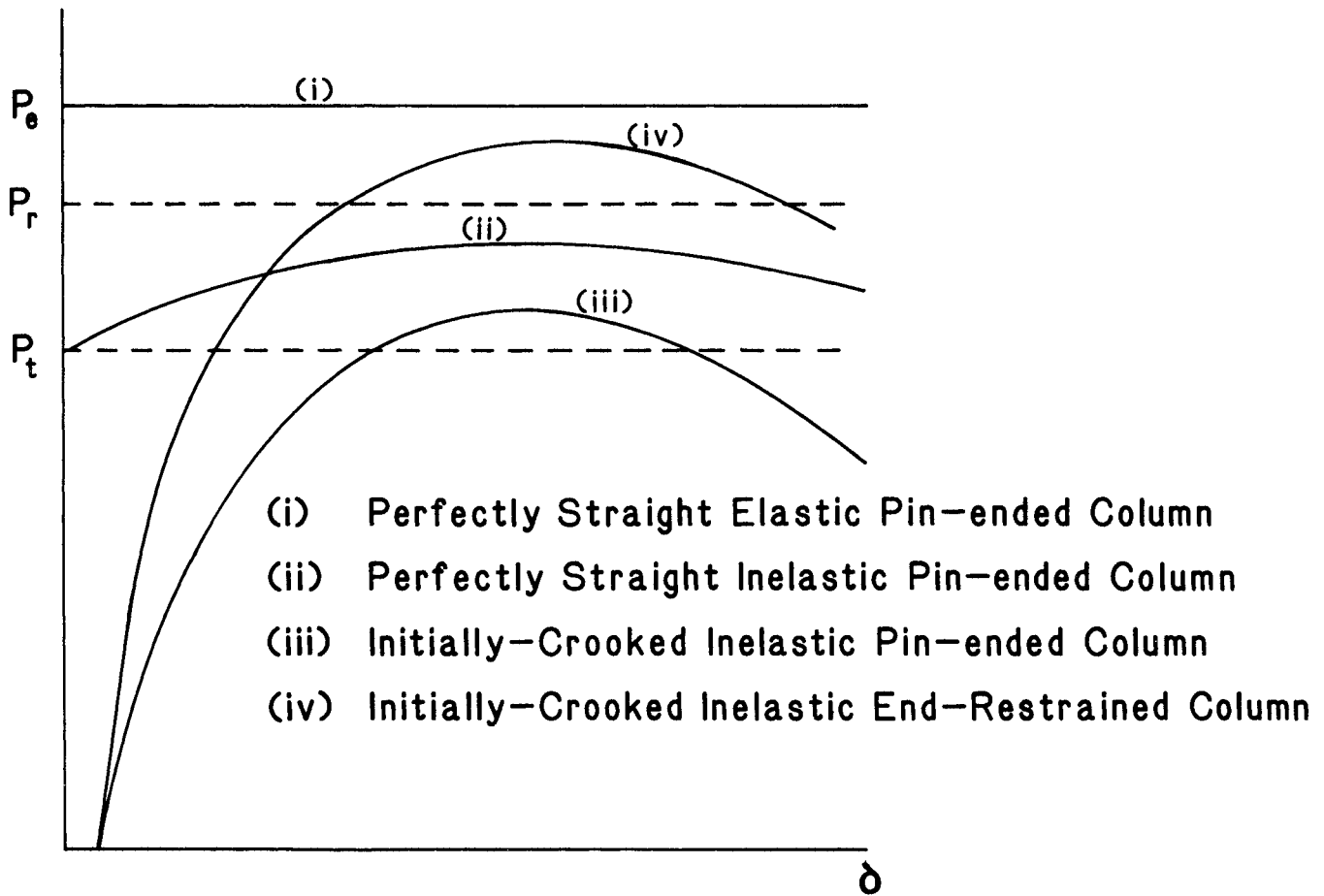


Fig. 4. Load-deflection behavior of columns

columns above the tangent modulus load. Using a simplified physical model, Shanley showed that bifurcation of equilibrium will take place when the applied load reaches the tangent modulus load. After bifurcation, increase in lateral deflection is accompanied by a slight increase in load above the tangent modulus load. Thus the maximum load is really slightly larger than the tangent modulus load, provided the column is perfectly straight. Extensions of Shanley's model to describe the buckling behavior of columns above the tangent modulus load were reported by Duberg and Wilder⁵ and Johnston.⁶

In Ref. 5, it was shown that if a column were artificially held in a straight position up to a load somewhere in between the tangent modulus and reduced modulus loads, then released, it would start to bend with an increase in axial load. The magnitude of the increase, however, was less than that of the tangent modulus load. If the column was held in a straight configuration up to the reduced modulus load, then released, it would bend with no increase in axial load. Reference 6 demonstrates that when a column buckles at the tangent modulus load there is no strain reversal only for an infinitesimal increment of axial load.

For any finite increase of axial load above the tangent modulus load, the column assumes equilibrium positions with increasing deflection accompanied by a strain reversal on the convex side of the column. Nevertheless, the amount of strain reversal is less than that of the reduced modulus theory. The readers are referred to a paper by Johnston⁷ for a more thorough discussion of the historic highlights of the column buckling theory.

The discussion so far pertains to columns which are perfectly straight. Columns in reality are rarely perfectly straight. Geometrical imperfection in a column tends to lower the maximum load of the member. As a result, the Structural Stability Research Council (formerly the Column Research Council) recommended the tangent modulus load be the representative failure load of a centrally loaded column.

The reduced modulus theory and the tangent modulus theory, as well as the Shanley's concept of inelastic column, are all based on physical reasoning. They provide solutions and explanations to the behavior of perfectly straight inelastic columns. The mathematical theory of elastic stability and the concepts of inelastic buckling are well explained in Refs. 8 and 9.

Plastic Stability—Numerical

As pointed out earlier, real steel columns not only exhibit inelasticity due to the presence of residual stresses, but also they possess initial crookedness. The analysis of columns with residual stresses and initial crookedness is rather complicated. The eigenvalue approach, which is valid only for perfectly straight columns, can not be used here. Instead, a different approach known as the stability approach must be utilized. In the stability approach, the load-deflection behavior of the column is traced from the start of loading to failure. The procedure is often carried out numerically using the computer because the differential equation governing the behavior of inelastic-crooked columns are often intractable, so closed form solutions are very difficult, if not impossible, to obtain. Various methods to obtain numerical solutions are presented in Refs. 10 and 11.

In addition to inelasticity and initial crookedness, the end conditions of a column also play an important role in affecting its behavior. The analyses of columns taking into consideration inelasticity, initial crookedness and end restraint were reported by a number of researchers in the past few years. The results are summarized in Ref. 12.

Structural Stability—Engineering

Columns in real structures seldom exist alone. The behavior of a column as an integral part of a structure is affected by the behavior of other structural members. In particular, in addition to carrying axial force, the column must be able to resist bending moments induced by the beam, so the column in reality behaves as a beam-column resisting both axial load and bending moments. The moment transfer mechanism between beams and columns is different depending on whether the connection is rigid or flexible. In other words, the behavior of the frame and its structural members is dependent on the rigidity of the connections. The stability analysis of frameworks with flexible connections has been a popular research topic in recent years. In particular, the recently published Load and Resistance Factor Design (LRFD) Specification¹³ designates two types of construction in its provision: Type FR (fully restrained) and Type PR (partially restrained) constructions. Type PR construction requires explicit consideration of connection flexibility in proportioning structural members.

The stability analysis of flexibly connected frames requires connection modeling. Since connection moment-rotation behavior is usually nonlinear, the inclusion of a connection as a structural element in a limit state analysis requires the use of nonlinear structural theory. With the advent of computer technology, great advancement has been made in computer-aided analysis and design of structures. At the present time, first- and second-order elastic analyses of structures can conveniently be performed for nearly all types of structures. Analysis of

structures loaded into the inelastic range can also be performed for certain types of structures.

The continued development in computer hardware and software has made it possible for engineers and designers to predict structural behavior rather accurately. The advancement in structural analysis techniques coupled with the increased understanding of structural behavior has made it possible for engineers to adopt the limit state design philosophy. A limit state is defined as a condition at which a structural member or its component ceases to perform its intended function under normal condition (serviceability limit state) or failure under severe condition (ultimate limit state). Load and Resistance Factor Design is based on the limit state philosophy and thus it represents a more rational approach to the design of structures.

This paper attempts to summarize the state-of-the-art methods in the analysis and design of columns as individual members and as members of a structure. A second objective is to introduce to engineers the stability design criteria of members and frames in LRFD. Highlights of recent research as well as directions of further research will be discussed.

2. PIN-ENDED COLUMN

A pin-ended column is the most fundamental case of a column. The behavior of a pin-ended column represents an anchorpoint for the study of all other columns. For columns with long slenderness ratio, the Euler formula (Eq. 1) will provide a good estimate of their behavior. For intermediate or short columns, the Euler formula has to be modified according to the reduced modulus concept or the tangent modulus concept (Eqs. 2 and 3) to account for yielding (or plastification) over the cross section due to the presence of residual stresses. As mentioned earlier, the tangent modulus theory gives a better prediction of inelastic column behavior and hence it is adopted for design purposes.

CRC Curve

Based on the study of idealized columns with linear and parabolic residual stress distribution, as well as the test results of a number of small and medium-size, hot-rolled, wide-flange shapes of mild structural steel, the Column Research Council recommended in the first edition of the Guide¹⁴ a parabola of the form

$$F_{cr} = F_y - B \left(\frac{KL}{r} \right)^2 \quad (4)$$

to represent column strength in the inelastic range. This parabola was chosen because it represented an approximate median between the tangent modulus strength of a W column buckled in the strong and weak directions. The column strength in the elastic range, however, is

represented by the Euler formula. The point of demarcation between inelastic and elastic behavior was chosen to be $F_{cr} = 0.5 F_y$. The number 0.5 was chosen as a conservative measure of the maximum value of compressive residual stress present in hot-rolled wide-flange shapes which is about $0.3 F_y$. To obtain a smooth transition from the parabola to the Euler curve, the constant B in Eq. 4 was chosen to be $F_y^2/4 \pi^2 E$. The slenderness ratio that corresponds to $F_{cr} = 0.5 F_y$ is designated as C_c in which

$$C_c = \sqrt{\frac{2\pi^2 E}{F_y}} \quad (5)$$

Thus, for columns with slenderness ratios less than or equal to C_c , the CRC curve assumes the shape of a parabola and for slenderness ratio exceeding C_c , the CRC curve takes the shape of a hyperbola, i.e.

$$F_{cr} = \begin{cases} F_y \left[1 - \frac{(KL/r)^2}{2C_c^2} \right] & \frac{KL}{r} \leq C_c \\ \frac{\pi^2 E}{(KL/r)^2} & \frac{KL}{r} > C_c \end{cases} \quad (6)$$

For comparison purposes, Eq. 6 is rewritten in its load form in terms of the nondimensional quantities P/P_y and λ_c in which P_y is the yield load given by $P_y = AF_y$ and λ_c is the slenderness parameter given by $\lambda_c = (KL/r) \sqrt{F_y/\pi^2 E}$

$$\frac{P}{P_y} = \begin{cases} 1 - 0.25\lambda_c^2 & \lambda_c \leq \sqrt{2} \\ \lambda_c^{-2} & \lambda_c > \sqrt{2} \end{cases} \quad (7)$$

The CRC curve is plotted in Fig. 5 in its nondimensional form (Eq. 7).

AISC/ASD Curve

The CRC curve divided by a variable factor of safety of

$$\frac{5}{3} + \frac{3}{8} \left(\frac{KL/r}{C_c} \right) - \frac{1}{8} \left(\frac{KL/r}{C_c} \right)^3$$

$$\left[= \frac{5}{3} + \frac{3}{8} \left(\frac{\lambda_c}{\sqrt{2}} \right) - \frac{1}{8} \left(\frac{\lambda_c}{\sqrt{2}} \right)^3 \right]$$

in the inelastic range and a constant factor of safety of 23/12 in the elastic range gives the AISC Allowable Stress

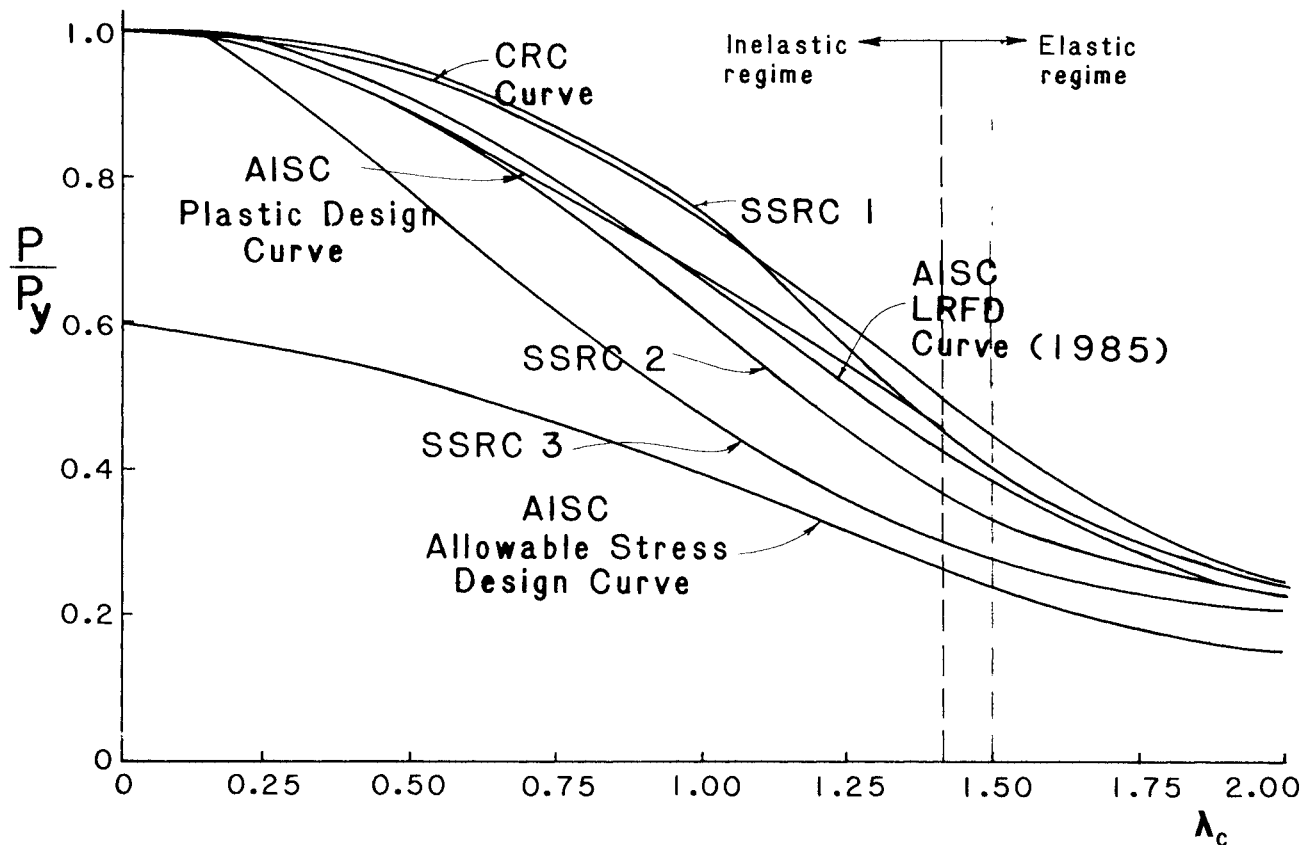


Fig. 5. Column design curves

Design (ASD) curve. The factors of safety are employed to account for geometrical imperfections and load eccentricities which are unavoidable in real columns. The AISC/ASD curve is also plotted in Fig. 5. The ASD column curve is used in conjunction with the ASD format given by

$$\frac{R_n}{F.S.} \geq \sum_{i=1}^j Q_{ni} \quad (8)$$

where

R_n = nominal resistance

(for column design, $R_n/F.S.$ is represented by the ASD column curve)

Q_n = service loads

AISC/PD Curve

The ASD curve multiplied by a factor of 1.7 forms the AISC Plastic Design (PD) curve (Fig. 5). In plastic design only the inelastic regime of the curve is utilized because of the slenderness requirement. The design format for plastic design of columns is thus

$$\frac{1.7R_n}{F.S.} \geq \gamma \sum_{i=1}^j Q_{ni} \quad (9)$$

where γ is the load factor used in the present AISC/PD Specification. The values for γ are: $\gamma = 1.7$ for live and dead loads only and $\gamma = 1.3$ for live and dead loads acting in conjunction with wind or earthquake loads.

SSRC Curves

Before proceeding any further, it should be stated that both the ASD curve and PD curve are originated from the CRC curve which was developed based on the bifurcation concept which postulates that the column is perfectly straight. Although residual stress is explicitly accounted for, the effect of geometrical imperfections is only accounted for implicitly by applying a variable factor of safety to the basic curve. Analysis of columns which explicitly take into consideration the effects of both residual stresses and initial crookedness was reported.¹⁵ The stability approach was used in the analysis and a set of three curves referred to as the SSRC multiple column curves¹⁶ was developed. Detailed expressions for these curves are given in Ref. 16. Approximate formulas for these curves based on physical reasoning which are useful for design are also reported.^{17,18}

For comparison purposes, the three SSRC curves are plotted with the CRC, ASD and PD curves in Fig. 5. These curves belly down in the intermediate slenderness range ($0.75 < \lambda < 1.25$) due to the combined maximum detrimental effects of both residual stresses and initial crookedness on column strength in the numerical analysis. Tests of real columns have demonstrated the det-

perimental effects of residual stresses and initial crookedness are not always synergistic, so the SSRC curves which belly down in the intermediate slenderness range will be too conservative for most columns in building frames.

AISC/LRFD Curve

To provide a compromise between the CRC curve (developed based on the tangent modulus concept) and the SSRC curves (developed based on the stability concept), the 1985 AISC/LRFD Specification¹³ adopted a curve of the form

$$\frac{P}{P_y} = \begin{cases} \exp < -0.419\lambda_c^2 & \lambda_c \leq 1.5 \\ 0.877\lambda_c^{-2} & \lambda_c > 1.5 \end{cases} \quad (10)$$

to represent basic column strength.

The LRFD curve is plotted on Fig. 5, together with the other curves described above. Note the LRFD curve lies between the CRC curve and the SSRC curve 2.

The LRFD format is

$$\phi R_n \geq \sum_{i=1}^j \gamma_i Q_{ni} \quad (11)$$

where

R_n = nominal resistance

Q_n = nominal load effects

ϕ = resistance factor

γ = load factor

Note the LRFD format has the features of both the ASD and PD formats in that factors of safety are applied to both the load and resistance terms to account for the variabilities and uncertainties in predicting these values. Furthermore, these load and resistance factors (ϕ , γ) are evaluated based on first order probabilistic approach. Since different types of loads have different degrees of uncertainties, different load factors are used for different types of loads (e.g. 1.6 for live load, 1.2 for dead load, etc.). Therefore, the LRFD format represents a more rational design approach.

The expressions for various column curves described above and the three state-of-the-art design formats (ASD, PD, LRFD) are summarized in Tables 1 and 2.

3. COLUMNS WITH END RESTRAINT

Eigenvalue Analysis

In addition to residual stresses and initial crookedness, the end conditions of a column have a significant influence on column behavior. For perfectly straight elastic columns with idealized end conditions (ideally pinned or fully rigid), an eigenvalue analysis can be carried out to determine the critical load P_{cr} . The effective length fac-

Table 1. Summary of Column Curves

Column Curves	Column Equations
CRC Curve	$\frac{P}{P_y} = 1 - \frac{\lambda_c^2}{4}$ $\lambda_c \leq \sqrt{2}$
	$\frac{P}{P_y} = \frac{1}{\lambda_c^2}$ $\lambda_c > \sqrt{2}$
AISC Allowable Stress Design Curve	$\frac{P}{P_y} = \frac{1 - \frac{\lambda_c^2}{4}}{\frac{5}{3} + \frac{3}{8} \left(\frac{\lambda_c}{\sqrt{2}}\right) - \frac{1}{8} \left(\frac{\lambda_c}{\sqrt{2}}\right)^3}$ $\lambda_c \leq \sqrt{2}$
	$\frac{P}{P_y} = \frac{12}{23} \frac{1}{\lambda_c^2}$ $\lambda_c > \sqrt{2}$
AISC Plastic Design Curve	$\frac{P}{P_y} = \frac{1.7 \left(1 - \frac{\lambda_c^2}{4}\right)}{\frac{5}{3} + \frac{3}{8} \left(\frac{\lambda_c}{\sqrt{2}}\right) - \frac{1}{8} \left(\frac{\lambda_c}{\sqrt{2}}\right)^3} \leq 1.0$ $\lambda_c \leq \sqrt{2}$
AISC LRFD Curve (1985 Version)	$\frac{P}{P_y} = \exp(-0.419\lambda_c^2)$ $\lambda_c \leq 1.5$
	$\frac{P}{P_y} = \frac{0.877}{\lambda_c^2}$ $\lambda_c > 1.5$

Table 2. Summary of Design Formats

Allowable Stress Design (ASD)	$\frac{R_n}{F.S.} \geq \sum Q_u$
Plastic Design (PD)	$R_n \geq \gamma \sum Q_u$
Load and Resistance Factor Design (LRFD)	$\phi R_n \geq \sum \gamma_i Q_u$

tor K for the column with the particular set of end conditions can be obtained by

$$K = \sqrt{\frac{P_e}{P_{cr}}} \quad (12)$$

where P_e is the Euler load given by $P_e = \pi^2 EI/L^2$ in which L is the length of the column.

The effective length factor multiplied by the true length L of the column gives the effective length of the column which can be used for design. Table 3¹⁹ gives the theoretical and recommended K values for columns with

Table 3. Theoretical and Recommended K Values for Idealized Columns

Buckled shape of column is shown by dashed line	(a)	(b)	(c)	(d)	(e)	(f)
Theoretical K value	0.5	0.7	1.0	1.0	2.0	2.0
Recommended design value when ideal conditions are approximated	0.65	0.80	1.2	1.0	2.10	2.0
End condition code						
					Rotation fixed and translation fixed	Rotation free and translation fixed
					Rotation fixed and translation free	Rotation free and translation free

various types of idealized end conditions. Since fully rigid supports are seldomly realized in real life, the recommended K values for cases with fixed support idealization are slightly higher than their theoretical values.

Numerical Analysis

It should be remembered that eigenvalue analysis can only be carried out for perfectly straight columns. For columns with initial crookedness, the stability or load-deflection approach must be used. In the load-deflection approach, the load-deflection behavior of the column is traced from the start of loading to collapse. The maximum load the column can carry is the peak point of the load-deflection curve. The analyses of non-sway columns with residual stresses, initial crookedness and small end restraint using the load-deflection approach have been reported by a number of researchers. The important results are summarized by the authors.¹² Some of the important findings are:

1. Comparing with pin-ended columns, the maximum load-carrying capacity of end-restrained columns increases as the degree of end restraint (as measured by the rotational stiffness of the connections connecting beams and columns) increases.
2. The increase in load-carrying capacity of end-restrained columns is more pronounced for slender columns when stability is the limit state than for short columns when yielding is the limit state.
3. The end-restraining effect on column strength is more noticeable for columns bent about their weak axes than for columns bent about their strong axes.
4. While residual stresses and initial crookedness have a destabilizing effect on columns strength, end restraint will provide a stabilizing effect which counteracts the detrimental effects of residual stresses and initial crookedness. However, the strengthening ef-

fect of end restraint is highly dependent on the slenderness of the column.

Practical Design of Initially Crooked Column with End Restraints

For design purposes, it is convenient to use the effective length factor approach in which the actual column with end restraints is converted to an equivalent pin-ended column by multiplying the actual unbraced length of the column by the effective length factor K , so the pin-ended column curves described in the preceding section can be utilized directly. The procedure to determine the effective length factor for initially crooked end-restrained columns with residual stresses is more involved than that of perfectly straight elastic columns with idealized end conditions. Equation 12 is not applicable anymore for the determination of the effective length factor K . Instead, a number of load-deflection curves, each corresponding to a specific slenderness ratio L/r (or slenderness parameter λ), are generated numerically. The peak points of these load-deflection curves are then plotted with the associated slenderness ratios (or slenderness parameters) to form a column curve (see Fig. 6). Each column curve is unique for a specific value of initial crookedness, a specific distribution of residual stress and a specific end restraint characteristic. To get the effective length factor, the end-restrained column curve (Fig. 6b) is compared with the corresponding pin-ended column curve and the K factor at any load level is given (Fig. 7),

$$K = \frac{\lambda_{ab}}{\lambda_{ac}} \quad (13)$$

where λ_{ab} , λ_{ac} are depicted in the figure.

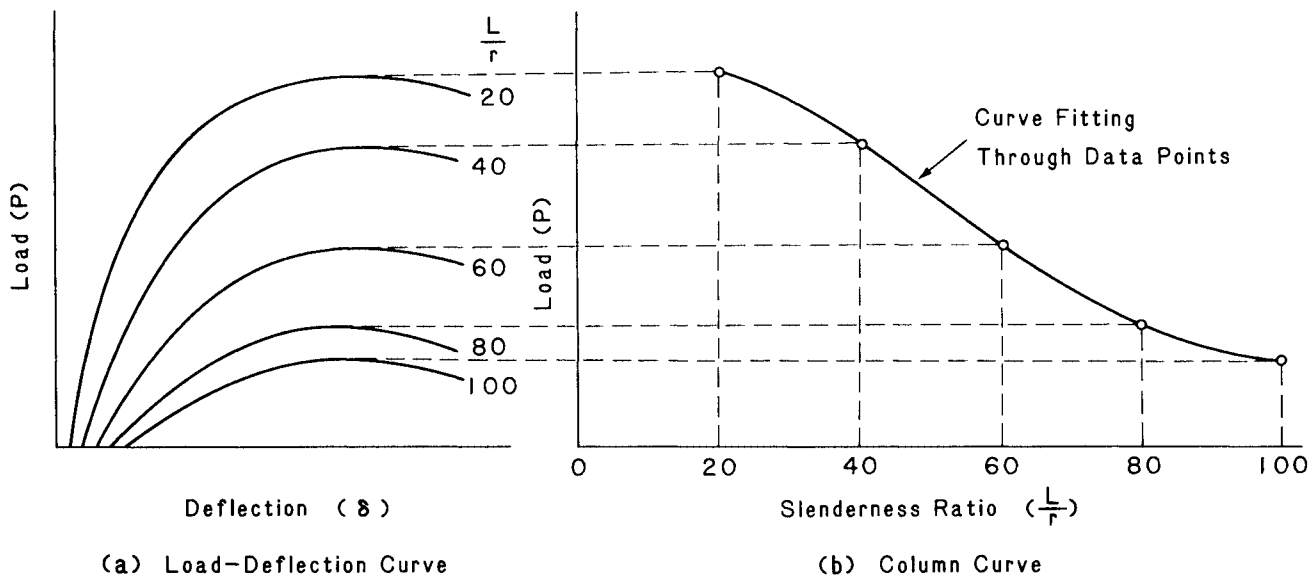


Fig. 6. Determination of column-strength curve from load-deflection curves for an initially crooked end-restrained column

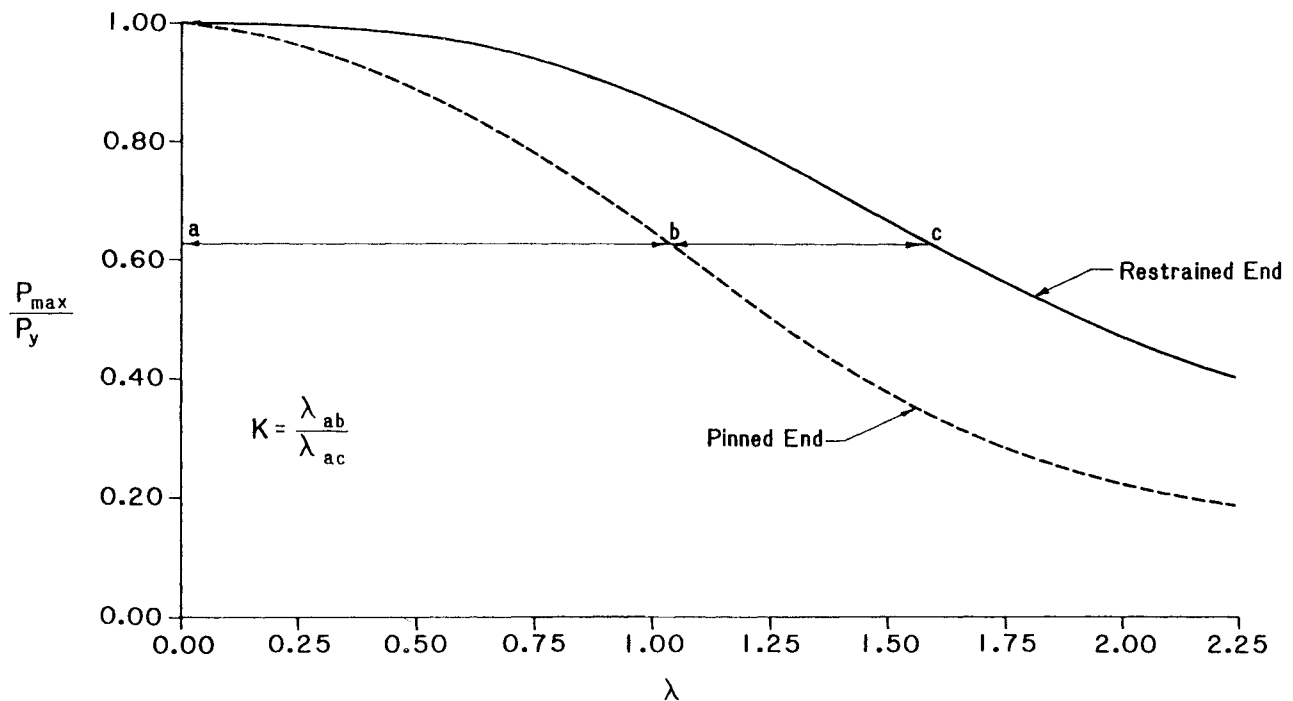


Fig. 7. Determination of effective length factor, K

Upon investigations of 83 end-restrained columns,²⁰ the values of K for each curve do not vary significantly over the load levels. Thus, a relationship between the K -factor and the magnitude of end restraint can be established. In particular, the expression

$$K = 1.0 - 0.017\bar{\alpha} \geq 0.6 \quad (14)$$

where

$$\bar{\alpha} = \frac{2EI_g}{(M_p)_c L_g} \left[\frac{1}{1 + \frac{2EI_g}{L_g R_{ki}}} \right] \quad (15)$$

in which

- I_g = moment of inertia of the girder connected to the column
- L_g = length of the girder
- $(M_p)_c$ = plastic moment capacity of the column
- R_{ki} = initial connection stiffness of the connection joining the beam to the column (Fig. 8)

was proposed¹² for non-sway columns with initial crookedness, residual stresses and small end restraints, taking into account the effect of beam flexibility. Procedures for the design of such columns have been reported in Refs. 12, 21 and discussed in Ref. 22.

At this point, it is interesting to compare the effective length factor K as described by Eq. 14 with the elastic effective length factor K_{el} determined by an eigenvalue

analysis assuming perfectly straight columns with end restraints provided by linear elastic rotational springs having spring stiffness R_{ki} at the ends. Such comparison is shown in Fig. 9. The dotted line is a plot of K versus $\bar{\alpha}$ whereas the solid lines are plots of K_{el} versus $\bar{\alpha}$. As can be seen, K_{el} gives a conservative estimate of column strength provided that λ is relatively low and $\bar{\alpha}$ is relatively high.

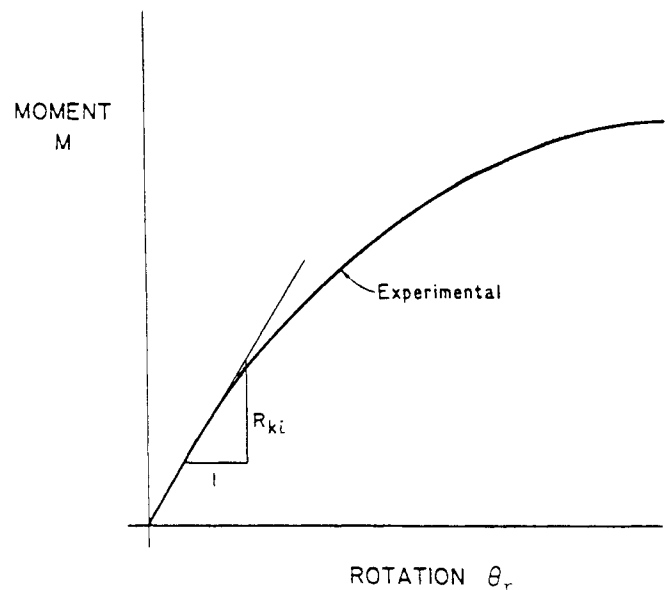


Fig. 8. Determination of R_{ki}

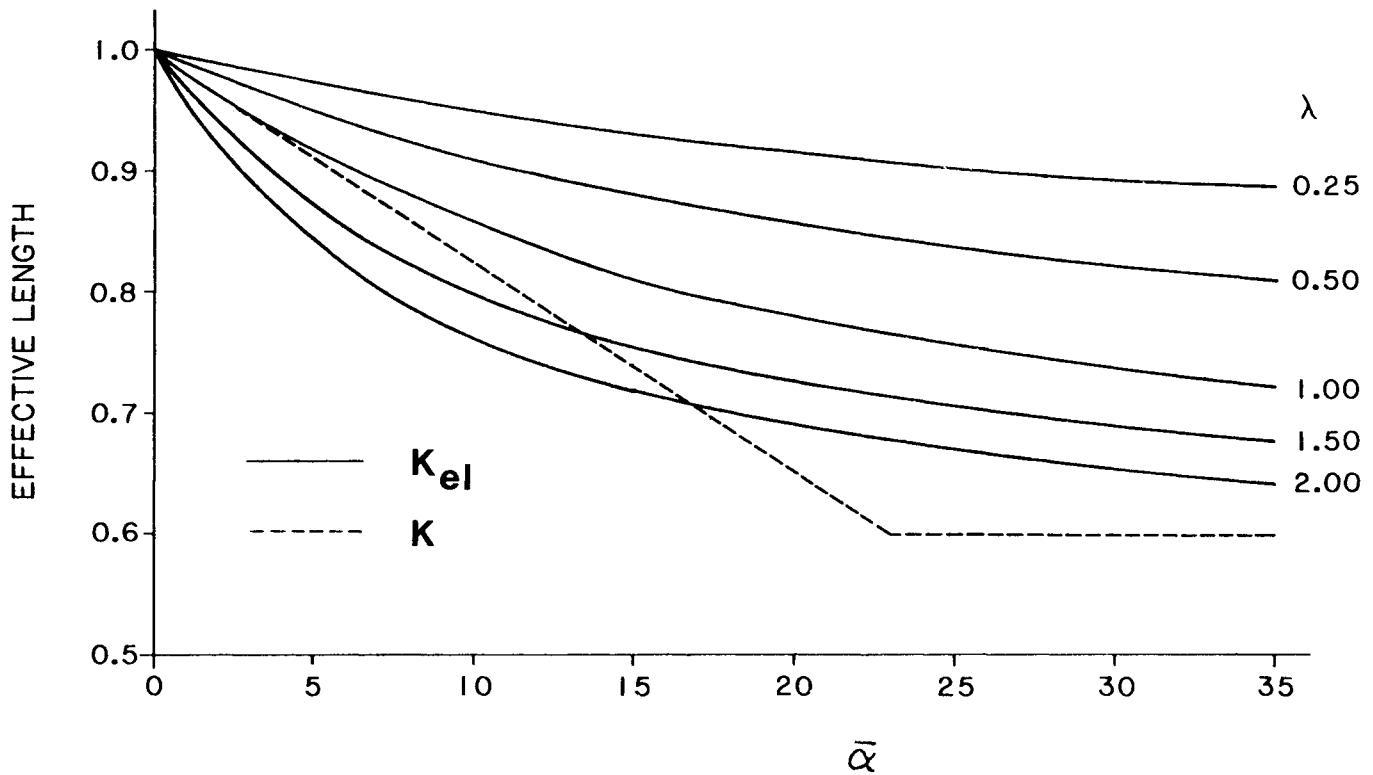


Fig. 9. Comparison of K_{el} and K

4. COLUMNS IN FRAMES

As mentioned earlier, columns in real structures usually exist as part of a frame. A column in a frame is usually subjected to the combined action of bending moments and axial thrust. As a result, part of the strength of the member is required to resist the bending moment and only the remaining part of the strength is available to resist the axial force. Thus, most columns in frames must be treated as beam-columns.

Columns in Braced Frames— B_1 Factor

A phenomenon associated with a beam-column is the secondary effect. When a braced member is subjected to both bending moments and axial force, the axial force acts through the deflection caused by the primary moments (moments arised from transverse loads and end moments acting on the member) to produce additional moment referred to as secondary or $P-\delta$ moment. Figure 10 shows schematically these two types of moments. The moment acting along the member is thus the algebraic sum of the primary and secondary moments. To obtain the exact value of this moment, a second-order analysis of the member is necessary. However, in lieu of such analysis, a simplified approach to obtain the total moment can be used.

Using the assumptions that

1. The deflection is small

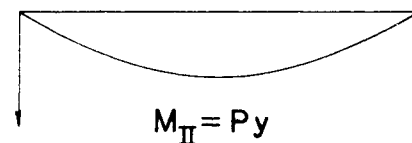
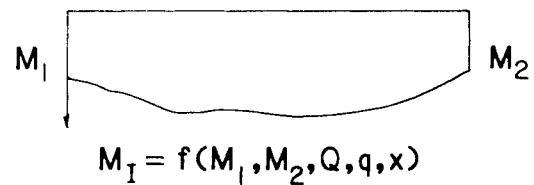
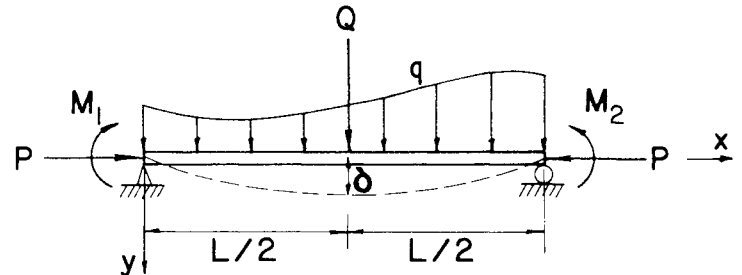


Fig. 10 $P-\delta$ effect

2. The secondary moment M_{II} is in the form of a half sine wave
3. The maximum deflection δ occurs at midspan
4. The maximum primary moment $M_{I_{max}}$ occurs at or near midspan

an approximate expression for the maximum moment can be derived.

Because of assumptions 1 to 3, we can relate the curvature caused by the secondary moment to the maximum deflection as

$$y''_{II} = -\frac{M_{II}}{EI} = -\frac{P\delta}{EI} \sin \frac{\pi x}{L} \quad (16)$$

Integrating Eq. 16 twice and enforcing the boundary conditions $y(0) = 0$ and $y(L) = 0$ it can easily be shown that the secondary deflection (deflection caused by the P - δ effect) can be written as

$$y_{II} = \frac{P\delta}{EI} \left(\frac{L}{\pi}\right)^2 \sin \frac{\pi x}{L} \quad (17)$$

from which the secondary deflection at midspan is

$$\delta_{II} = y_{II} |_{x=L/2} = \frac{L}{2} = \delta \frac{P}{P_e} \quad (18)$$

Since the total deflection at midspan is the sum of the primary and secondary deflections, i.e.

$$\delta = \delta_I + \delta_{II} \quad (19)$$

we can eliminate δ_{II} by substituting Eq. 18 into Eq. 19. The result is

$$\delta = \frac{\delta_I}{\left(1 - \frac{P}{P_e}\right)} \quad (20)$$

From assumption 4, we can write

$$M_{max} = M_{I_{max}} + P\delta \quad (21)$$

If we substitute Eq. 20 into Eq. 21 and rearrange, we can write

$$M_{max} = \left[\frac{C_m}{1 - P/P_e} \right] M_{I_{max}} = B_1 M_{I_{max}} \quad (22)$$

where

$$B_1 = \frac{C_m}{1 - P/P_e} \geq 1 \quad (23)$$

$$C_m = 1 + \psi P/P_e$$

in which

$$\psi = \frac{\delta_I P_e}{M_{I_{max}}} - 1 \quad (24)$$

Equation 22 shows the maximum moment in the member can be obtained by multiplying the maximum primary moment $M_{I_{max}}$ by an amplification factor B_1 (the factor in parenthesis). Note this amplification factor must be greater than unity if it is of any importance. This is because if this factor is less than unity, then from Eq. 22 it is clear that $M_{I_{max}} > M_{max}$ and the designer will use $M_{I_{max}}$ rather than M_{max} in proportioning the members. The condition that B_1 must be greater than unity is adopted in the present AISC/LRFD Specification which was not the case for the AISC/ASD Specification.

Figure 11 shows the value of ψ and C_m for several different load cases. It is important to point out that because of assumption 4, Eq. 24, which is derived from Eq. 21, is only applicable to the two simply supported cases (Cases 1 and 4). For the other cases in which the maximum primary moment $M_{I_{max}}$ occurs at the end(s) (Cases 2, 3, 5) or occurs at midspan as well as at the ends (Case 6), the exact values of the maximum moments are first evaluated; the values for ψ are then obtained from calibration.²³

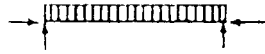
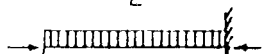
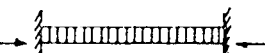
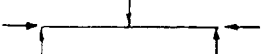
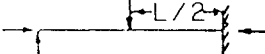
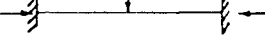
Case	ψ	C_m
1 	0	1.0
2 	-0.4	$1 - 0.4 P/P_e$
3 	-0.4	$1 - 0.4 P/P_e$
4 	-0.2	$1 - 0.2 P/P_e$
5 	-0.3	$1 - 0.3 P/P_e$
6 	-0.2	$1 - 0.2 P/P_e$

Fig. 11. Values of ψ for beam-columns under transverse loadings

For the cases in which end-restraint(s) is (are) present (Cases 2, 3, 5, 6), the value of C_m for usual P/P_e ratios is only slightly less than unity and a conservative value of 0.85 is thus suggested for C_m . For the two simply supported cases (Cases 1, 4), a value of 1 is suggested for C_m in the AISC/LRFD Specification.¹³

A special case arises when in-span transverse loads are absent in the member. For this case, the primary moment in the member is caused by end moments acting on the member ends. Since the maximum primary moment in members subjected to axial load and end moments seldom exists at midspan, C_m defined in Eq. 23 is invalid since it was developed based on assumption 4 postulating that $M_{I_{max}}$ occurs at or near midspan. Instead, C_m is redefined as

$$C_m = 0.6 - 0.4 (M_1/M_2) \geq 0.4 \quad (25)$$

where M_1/M_2 is the ratio of the smaller to larger end moments of the unbraced length of the member and it is positive when the member is bent in reverse curvature and negative when the member is bent in single curvature.

Equation 25 was developed based on the equivalent moment concept. In the equivalent moment model, a pair of equal and opposite end moments are applied to the member which, when amplified by the amplification B_1 , will give the same maximum moment as will the actual unequal end moments. It is obvious the location of maximum moment will be distorted, but this is ignored for simplicity. C_m expressed in Eq. 25 was proposed by Austin²⁴ based on a more accurate expression derived by Massonnet.²⁵

Columns in Unbraced Frames— B_2 Factor

The above discussion on moment amplification pertains to members in braced frames in which sidesway is prevented. For members in an unbraced frame, in addition to $P-\delta$ effect there is another effect known as the $P-\Delta$ effect. The $P-\Delta$ effect arises when the gravity loads of a frame act through the drift of the frame thus producing additional overturning moment and additional drift (Fig. 12). Since this is a destabilizing effect, it should be considered in design. Both the $P-\delta$ and $P-\Delta$ effects can be taken into account by using second-order analysis. The AISC/LRFD Specification¹³ recommends the use of $P-\Delta$ moment amplification factor B_2 to account for the $P-\Delta$ effect in lieu of a second-order analysis.

Two expressions for B_2 are given in the specification

$$B_2 = \frac{1}{1 - \frac{\sum P_u \Delta_{oh}}{\sum HL}} \quad (26)$$

and

$$B_2 = \frac{1}{1 - \frac{\sum P_u}{\sum P_e}} \quad (27)$$

where

$\sum P_u$ = design axial forces on all columns of a story, in kips

Δ_{oh} = translation deflection on the story under consideration based on a first-order analysis, in inches

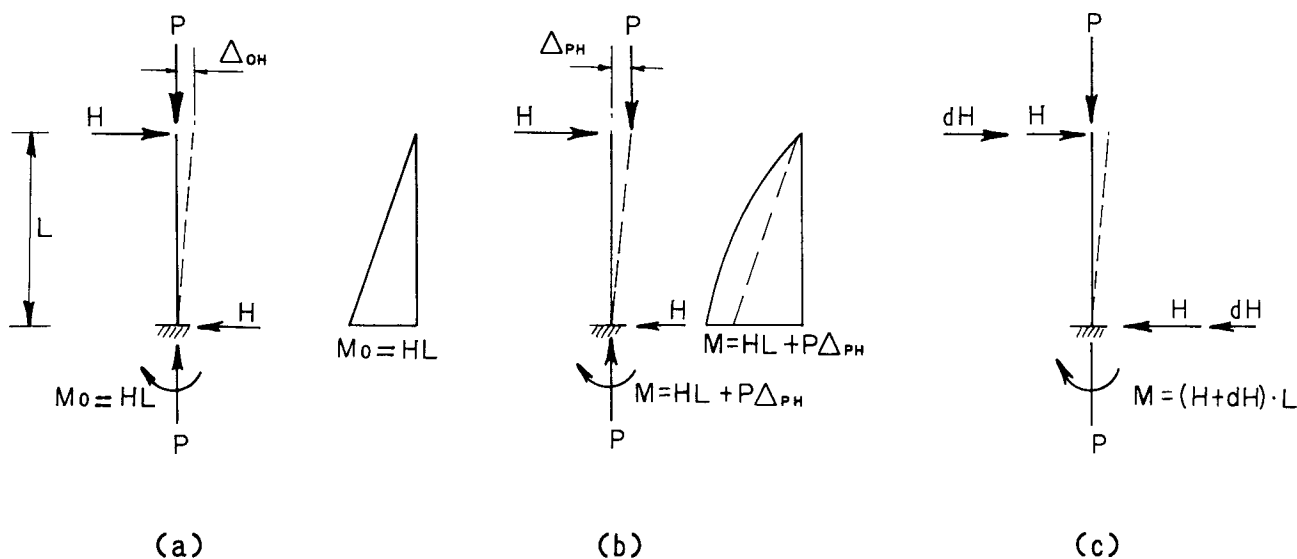


Fig. 12. Cantilever column

- ΣH = sum of all story horizontal forces producing Δ_{oh} , in kips
 L = story height, in inches
 P_e = Euler load (Eq. 1)

Equation 26 was developed based on the story stiffness concept.^{26,27,28} By assuming that

1. each story behaves independently of other stories, and
2. the additional moments in the columns caused by the P - Δ effect is equivalent to that caused by a lateral force of $\Sigma P_u \Delta / h$ where ΣP_u is the sum of all vertical forces on the story, Δ is the total frame drift including the P - Δ effect and h is the height of the story,

the sway stiffness of the story can be defined as:

$$S_F = \frac{\text{horizontal force}}{\text{lateral displacement}} \quad (28)$$

$$= \frac{\Sigma H}{\Delta_{oh}} = \frac{\Sigma H + \Sigma P \Delta / h}{\Delta}$$

Solving the above equation for Δ gives

$$\Delta = \left(\frac{1}{1 - \frac{\Sigma P \Delta_{oh}}{\Sigma H h}} \right) \Delta_{oh} \quad (29)$$

If rigid connections and elastic behavior are assumed, the magnified moment induced in the member as a result of sway M_{lt} will be proportional to the lateral deflections. Therefore, we can write

$$(M_{lt})_{max} = \left(\frac{1}{1 - \frac{\Sigma P \Delta_{oh}}{\Sigma H h}} \right) M_{lt} = B_2 M_{lt} \quad (30)$$

where

M_{lt} = moment due to lateral translation determined from a first-order analysis

The alternative expression for the moment amplification factor B_2 is obtained as a direct extension of Eq. 20. Under the assumption that when sidesway instability is to occur in a story, all columns in that story will become unstable simultaneously, the P/P_e term in Eq. 20 is replaced by $\Sigma P_u / \Sigma P_e$ in which the summation is carried through all columns in a story.²⁹ Using the same argument as before that if elastic behavior and rigid connections are assumed, the story sway moment will be proportional to the lateral deflection. As a result, the maximum end moment accounting for the P - Δ effect can be written as

$$(M_{lt})_{max} = \left(\frac{1}{1 - \frac{\Sigma P_u}{\Sigma P_e}} \right) M_{lt} = B_2 M_{lt} \quad (31)$$

The P - Δ moment amplification factor B_2 described above and recommended in the AISC/LRFD Specification represents an improvement over that recommended in the AISC/ASD Specification¹⁹ in which the P - Δ moment amplification factor is expressed as $0.85/(1 - f_d/F'_e)$. The reason is that the B_2 factor in the LRFD Specification magnifies only the sway moment M_{lt} , whereas the moment amplification factor in the ASD Specification magnifies the total moment. If the bulk of the column moment does not produce sidesway, the approach recommended in the ASD Specification will be unduly conservative.

Column Design in LRFD for Type FR Construction

As mentioned earlier, for an unbraced frame, both the P - δ and P - Δ effects are important, so both effects have to be accounted for in design. The AISC/LRFD Specification recommends a superposition technique in which the P - δ (sometimes called the member instability) effect and the P - Δ (sometimes called the frame instability) effect are summed together algebraically to obtain the maximum design moment, i.e.

$$M_u = B_1 M_{nt} + B_2 M_{lt} \quad (32)$$

where B_1 and B_2 are the P - δ and P - Δ moment amplification factors respectively and M_{nt} is the moment in the member assuming there is no lateral translation in the frame and M_{lt} is the moment in the member as a result of lateral translation of the frame.

In the actual design, M_{nt} is determined from a first-order analysis of the frame braced against lateral translation under the applied loads. M_{lt} is determined from a first-order analysis of the frame acted on by the reverse of the bracing forces (Fig. 13). It is important to note Eq. 32 is a conservative approach, since the maximum P - δ moment and the maximum P - Δ moment may not necessarily coincide at the same location. Furthermore, it should be remembered the expressions for B_1 and B_2 are only valid if the joints are rigid. In other words, Eq. 32 is only applicable to Type FR (fully restrained) construction in the LRFD Specification. Finally, it should also be mentioned that, depending on how the frame is braced against sway, the moments M_{nt} and M_{lt} calculated will be different for different arrangements of fictitious supports. However, for regular rectangular frames used in most building construction, the difference is insignificant for design purpose.

The validity of Eq. 32 has been checked by comparing the maximum moment calculated using Eq. 32 with the exact maximum moment calculated using a second-order elastic analysis.³⁰ It is concluded that for rectangular frames in which the P - Δ effect is not too significant, good correlation between the two calculated moments is observed.

Furthermore, if the P - Δ effect is not too significant,

the two different expressions for B_2 (Eqs. 26 and 27) give comparable results provided that all the beams and columns in the story are rigidly connected.

If the P - Δ effect is significant, viz, if $B_2 > 1.5$, the approach suggested by LeMessurier³¹ provides more accurate results. In his approach, the moment magnification factor is expressed as

$$B_2 = \frac{1}{1 - \frac{\sum P_u}{\sum P_L - \sum C_L P}} \quad (33)$$

where

$$\sum P_L = \frac{\sum Hh}{\Delta_{oh}} \quad (34)$$

C_L is a factor accounting for the decrease in stiffness of the column due to the presence of the axial force.

Note that if C_L is insignificant, Eq. 33 reduces to Eq. 26.

5. CONNECTION RESTRAINT CHARACTERISTICS

The analyses and design of Type FR (fully restrained) and Type PR (partially restrained) frames differ in that for Type PR construction, the effect of connection flexibility must be taken into account. Since a connection is a highly statical indeterminate element, a rigorous analytical study of its behavior is quite a formidable task. In view of this, a special Task Group (TG25) of the Structural Stability Research Council was set up to investigate theoretically and experimentally connection behavior.

The behavior of a connection is best described by its moment-rotation relationship. Since most connection moment-rotational relationships are nonlinear almost from

the start of loading, the analysis of structures including the effect of connection flexibility is an inherent nonlinear problem. To simplify the analysis technique, a number of simplified models have been proposed.

Connection Modeling

Figure 14 shows two simple linear models. The first model³² uses the initial stiffness R_{ki} of the connection to represent the behavior of the connection for the entire range of loading. As can be seen, the validity of this

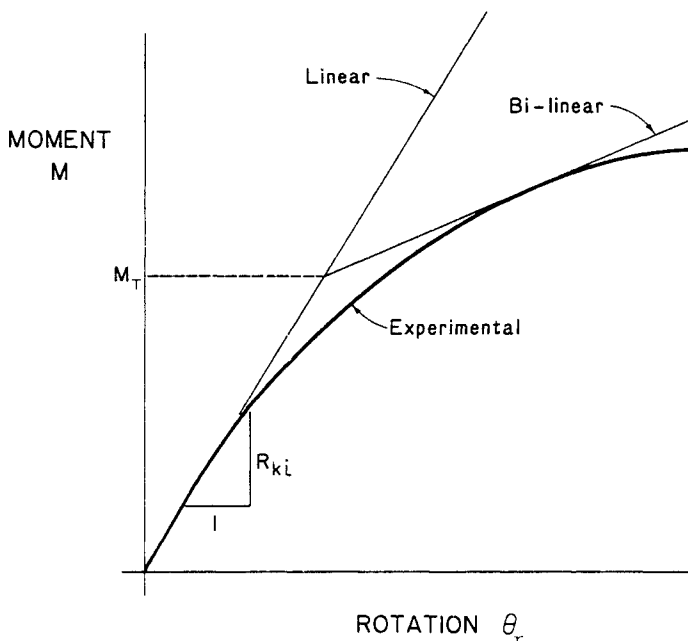


Fig. 14. Linear M - θ , models

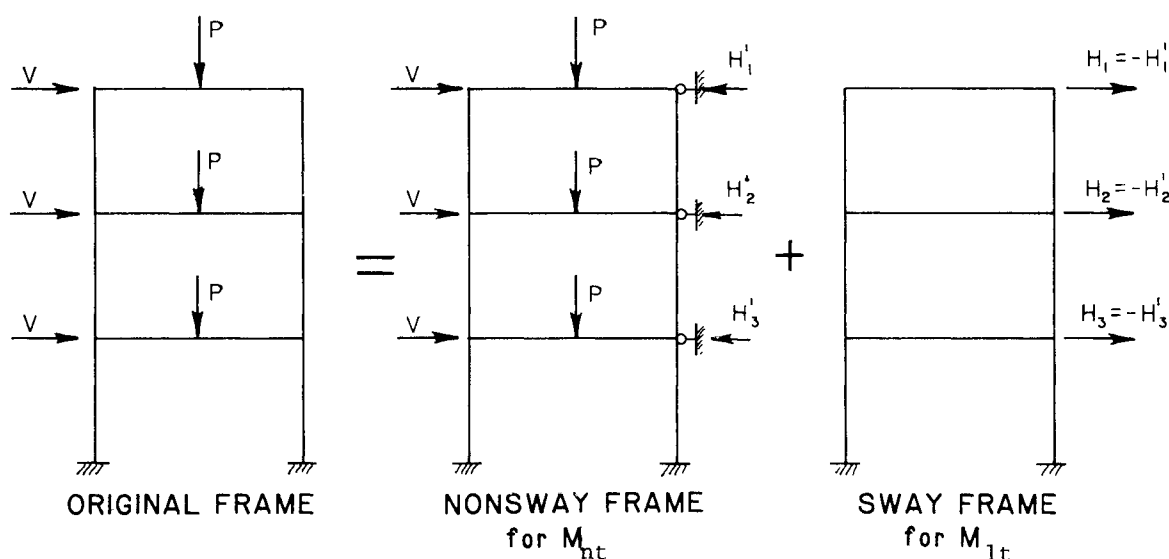


Fig. 13. Two fictional frames for M_{nt} and M_{1t}

linear model deteriorates as the moment increases. To get a better representation of the connection stiffness, a bilinear model³³ was used. In the bilinear model, the initial slope of the moment-rotational line was replaced by a shallower line at a certain transition moment M_T . A direct extension of the bilinear model is the piecewise linear model³⁴ in which the nonlinear $M-\theta_r$ curve of the connection is represented by a series of straight line segments. Although the linear, bilinear or piecewise linear models are easy to implement, the inaccuracies and sudden jump in stiffness which are inherent in these models make them undesirable to be used in a limit state analysis routine.

To this end, Frye and Morris³⁵ proposed a polynomial model in which a polynomial is used to represent the connection $M-\theta_r$ behavior (Fig. 15). However, there is a major drawback in this model. Since the nature of a polynomial is to peak and trough within a certain range, the stiffness of the connection (as represented by the first derivative of the polynomial) may be negative, which is physically unjustifiable. To overcome this, Jones et al³⁶ uses a cubic B -spline curve fitting technique to improve the polynomial model (Fig. 15). In the cubic B -spline

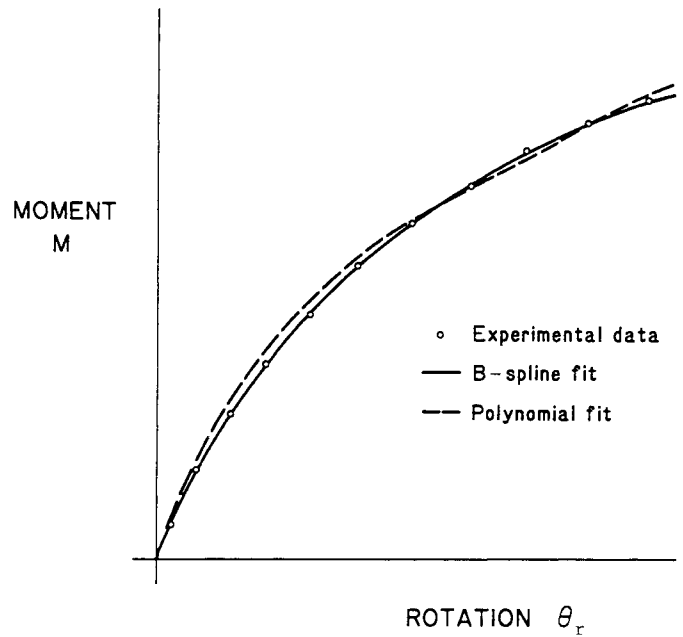


Fig. 15. B -spline and polynomial curve fit models

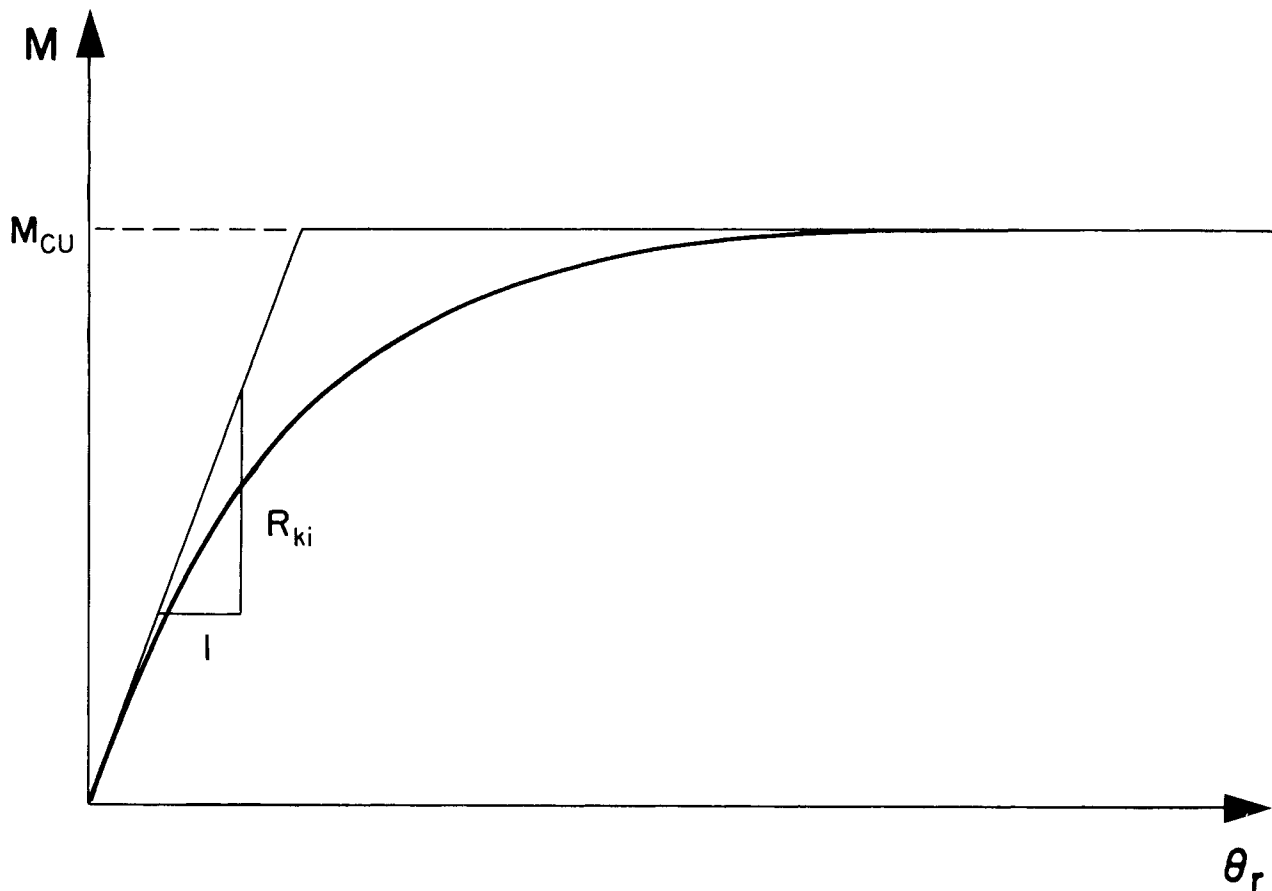


Fig. 16. Connection moment-rotation idealization used in the power model

model, a cubic polynomial is used to curve-fit segments of a curve. Continuity between the first and second derivatives of each segment of curve are enforced. Although the cubic *B*-spline model gives a good representation of the connection behavior and circumvents the problem of negative stiffness, a large number of data are necessary for the curve-fitting process. To overcome this, the power model proposed by Colson³⁷ and the exponential model proposed by Lui³⁸ can be used.

In the power model,³⁷ a power function is used to represent the connection *M*- θ_r behavior. It has the form

$$\theta_r = \frac{|M|}{R_{ki}} \frac{1}{1 - \left| \frac{M}{M_{cu}} \right|^a} \quad (35)$$

where (refer to Fig. 16)

- R_{ki} = initial connection stiffness
- M_{cu} = ultimate moment capacity of the connection
- a = a parameter to account for the curvature of the *M*- θ relationships

In the exponential model,³⁸ the connection *M*- θ_r behavior is represented by an exponential function of the form

$$M = \sum_{j=1}^n C_j (1 - e^{-|\theta_r|/2j^\alpha}) + M_o + R_{kf} |\theta_r| \quad (36)$$

where

- M_o = initial moment
- R_{kf} = final or strain-hardening connection stiffness
- α = scaling factor
- C_j = connection model parameters

The connection model parameters are merely curve-fitting constants which can be obtained by using an optimization technique.

To demonstrate the validity of the exponential model, two experimentally obtained moment-rotation curves are curve-fitted with Eq. 36 using four curve-fitting constants and 10 sets of data from each curve. The results are shown in Figs. 17 and 18 respectively. The connection used in Fig. 17 was a double web angle connection tested by Lewitt, Chesson and Munse.³⁹ The connection used in Fig. 18 was a T-stub connection tested by Rathbun.³² As can be seen, the exponential model gives an excellent representation of the test curves.

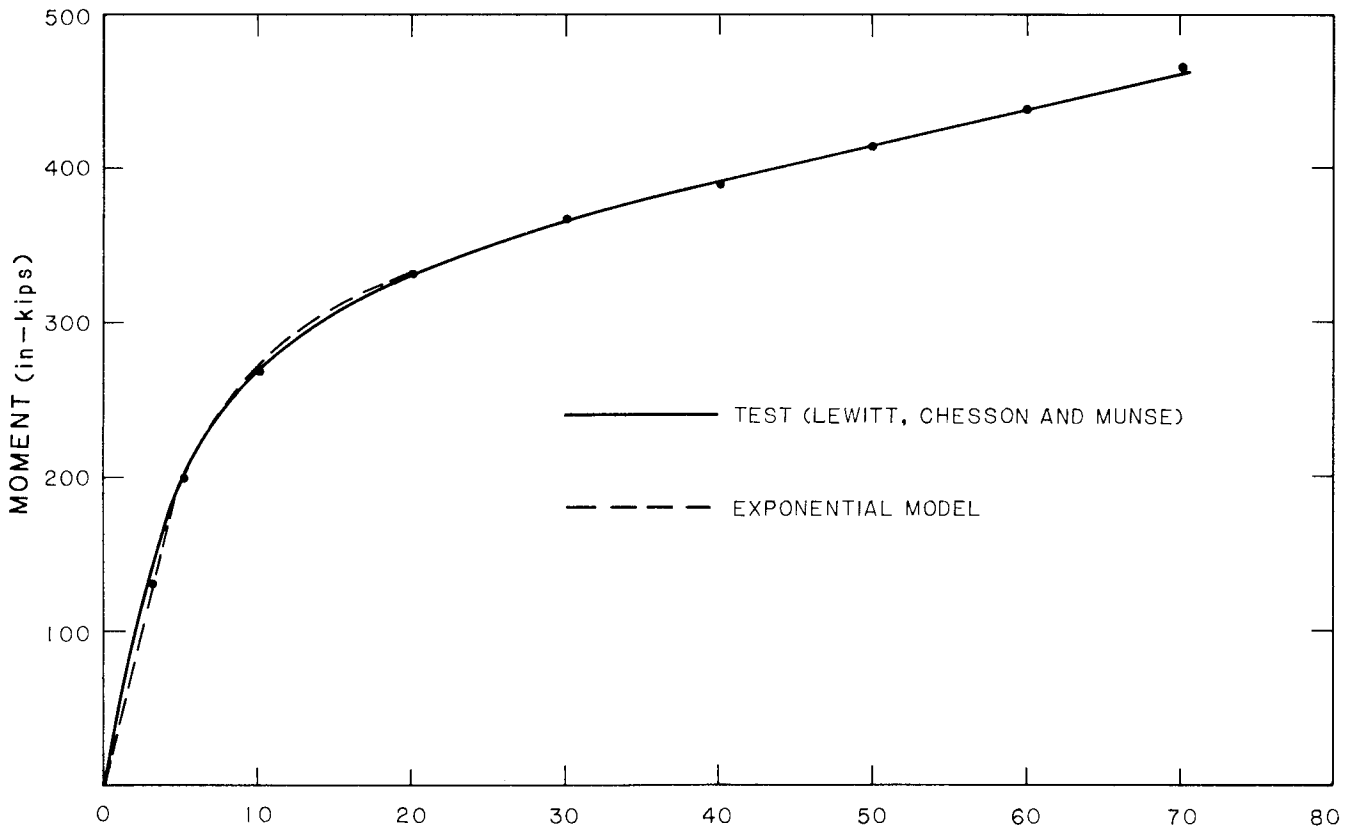


Fig. 17. Comparison of exponential connection model with test by Lewitt, Chesson and Munse

Research Need

As mentioned earlier, because of the complex geometries and stress distributions of most connections, most $M-\theta$ curves are nonlinear and thus almost all existing $M-\theta$ curves available today are obtained from experiments. Since most of these experiments were performed on connections which have become obsolete, it is essential that additional analytical and experimental investigations on commonly used connections be conducted in view of the advancement made on the limit state approach to analysis and design of steel structures.

6. BEHAVIOR OF COLUMNS WITH RIGID AND SEMI-RIGID CONNECTIONS

For columns in frames, another important phenomenon which the engineers should be aware of is the moment transfer mechanism between the beams and columns. One commonly posed question is: how can a beam restrain a column if at the same time it is inducing moment to the column? Whether a beam restrains or induces moment to the column depends on a number of factors. Some of the important ones are (1) the rigidity of the connections, (2) the relative stiffness of the beams and columns and (3) the load patterns and load sequences on the frame.

Moment Transfer—Rigid Connection

To study the moment transfer mechanism between the beam and the column, it is advantageous to look at the behavior of some simple subassemblages. Figure 19⁴⁰ shows a T-shaped subassemblage consisting of two beams and a column rigidly connected to one another. A concentrated load Q equal to half the yield load of the beam is applied to the midspan of each beam, an axial load P is then applied to an imperfect column with the influence of residual stress as well as with an initial out-of-straightness of $0.001L$. The moment distributions of the joint are plotted as P increases. By assuming that the beams behave elastically for the entire range of loading and the joint is rigidly connected, the moment at the joint is considered to consist of three parts:

1. Bending moment M_1 due to lateral load Q with joint fixed.
2. Bending moment M_2 due to joint translation as column buckles.
3. Bending moment M_3 due to joint rotation.

These three components of bending moments are shown schematically in Fig. 20.

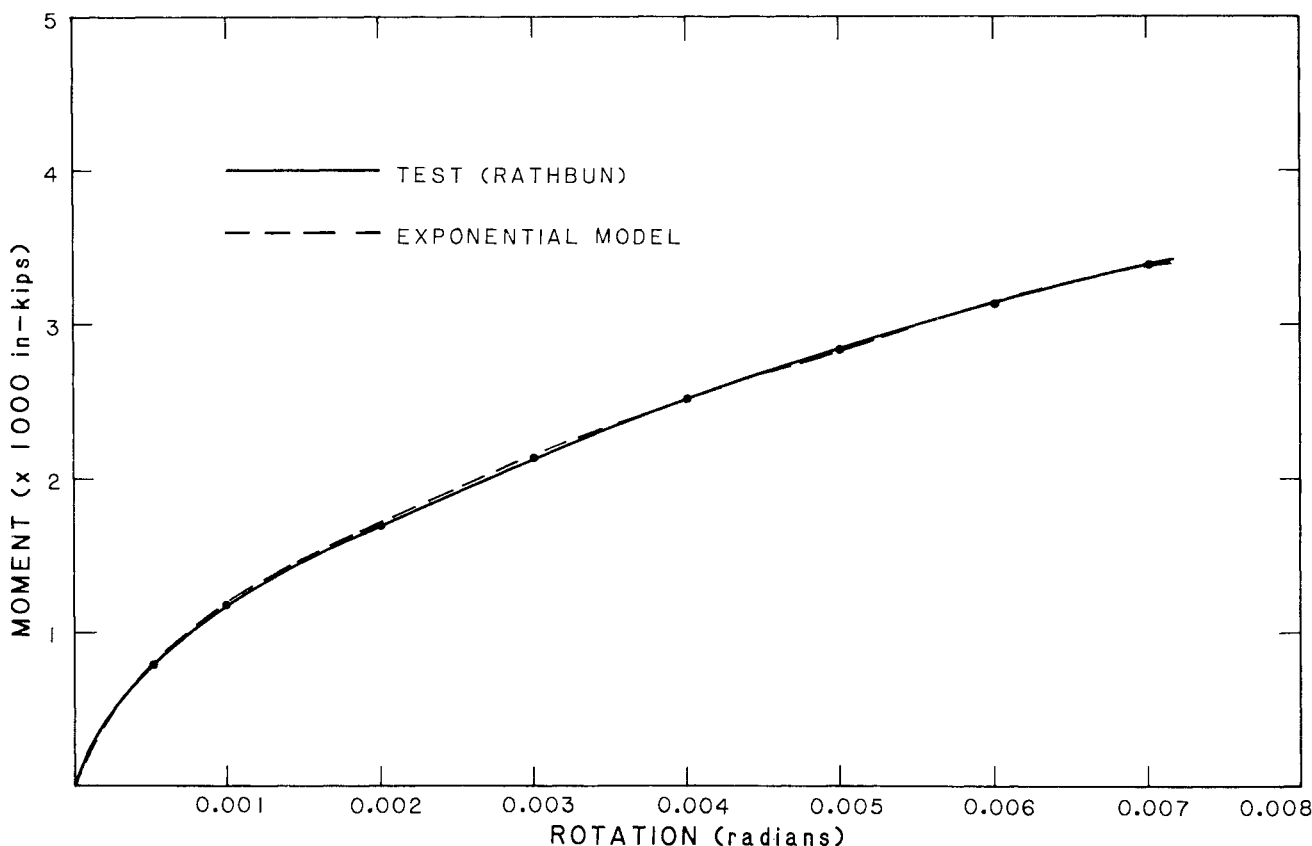


Fig. 18. Comparison of exponential connection model with test by Rathbun

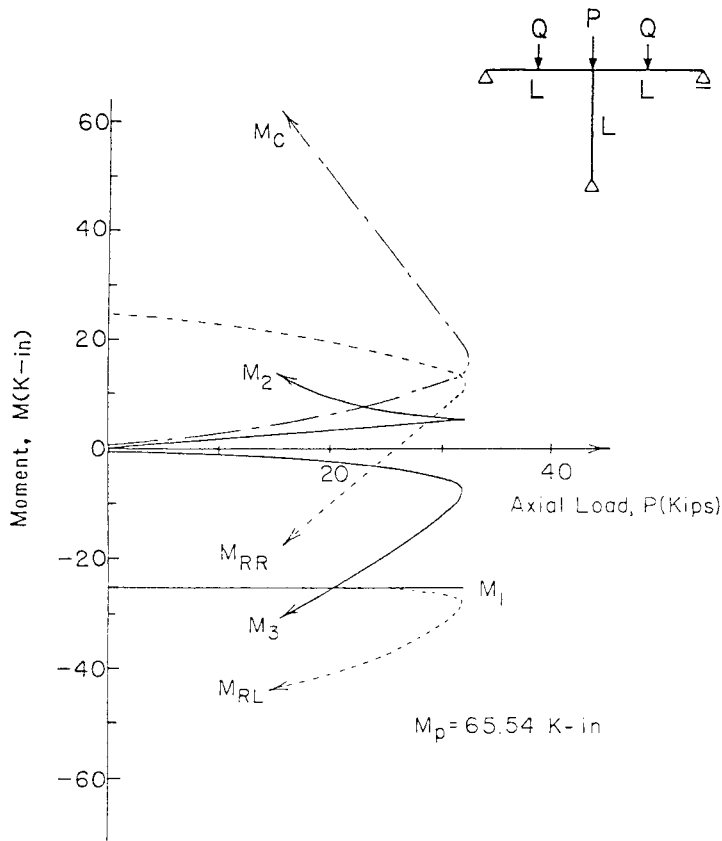


Fig. 19. Moment distributions at joint of subassembly

The bending moments in the left beam M_{RL} and in the right beam M_{RR} can be expressed as follows:

$$M_{RL} = -M_1 + M_2 - M_3 \quad (37)$$

$$M_{RR} = M_1 - M_2 - M_3 \quad (38)$$

The bending moment in the column M_C can be obtained by considering joint equilibrium.

$$M_C = -(M_{RL} + M_{RR}) = 2M_3 \quad (39)$$

The variation of these bending moments with the axial load P is plotted in Fig. 19. It can be seen from the figure that the moment due to the buckling of the column is not negligible. Not only does it reduce the moment of the left beam, but, together with the moment arising from joint rotation, restrains the column during the final stage of loading. The moment of the right beam M_{RR} , at first inducing moment to the column, decreases gradually and at $P = 26$ kips reverses sign and becomes a restraining moment to the column. On the other hand, the moment of the left beam M_{RL} is always negative and thus always restrains the column.

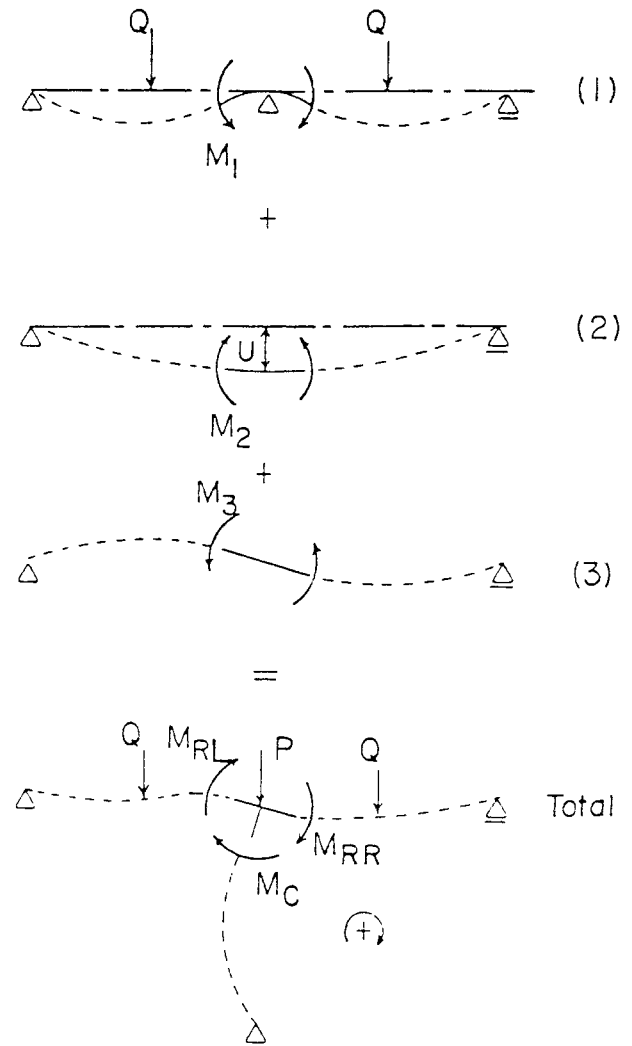


Fig. 20. Components of bending moments at joint of subassembly

Moment Transfer—Flexible Connection

If the connections are not rigid, the moment transfer mechanism between the beam and the column are more complicated because of the loading/unloading characteristic of the connections. To demonstrate this characteristic schematically, the readers are referred to Fig. 21. For this subassembly (Fig. 21a), the beams are connected to the column by semi-rigid connections. Beam loads w_L , w_R are first applied to simulate the dead load of the structure. Figure 21b shows the directions of moments acting on the left- and right-hand side of the joint of the subassembly. The corresponding $M-\theta$, curves for the left and right connections are also shown. The left connection will follow curve OA' and the right connections will follow curve OA'' . The moment acting on the column will be M_{1L} on the left side of the joint and M_{1R} on the right side of the joint.

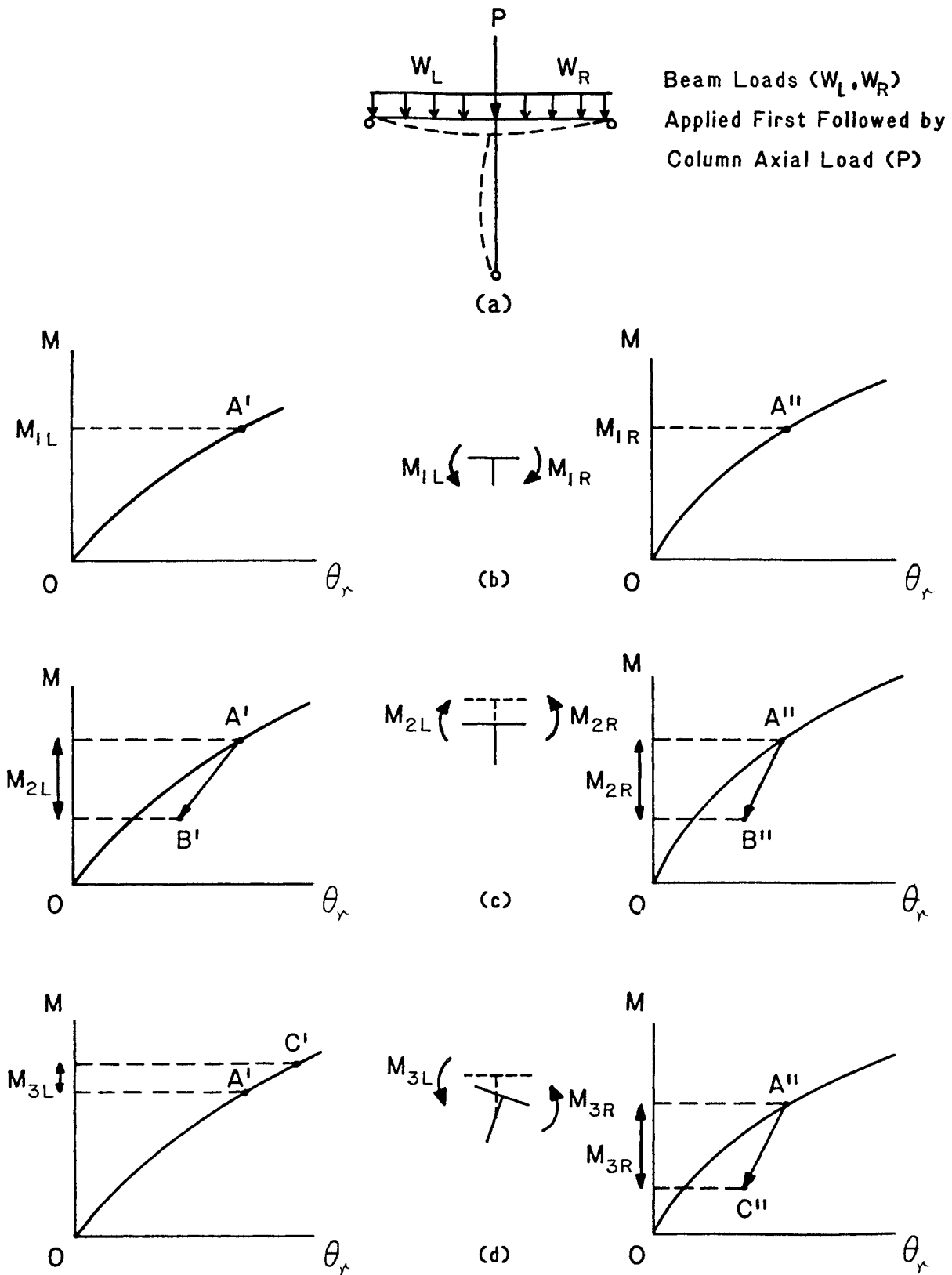


Fig. 21. Schematic representation of moment transfer mechanism of a flexibly connected subassembly

Now, a column axial load P is applied to the subassembly to simulate the live load. Under the action of P , the column will shorten and bend as shown by the dashed line in Fig. 21a. The moment induced due to shortening of the column is shown in Fig. 21c. Note that the directions of moments on both sides of the column are opposite to that of Fig. 21b. Therefore, unloading of the connections will result. As a result, the $M-\theta_r$ curve of the left connection will follow path $A'B'$ and that of the right connection will follow path $A''B''$. The slopes of $A'B'$ and $A''B''$ are parallel to the initial slopes to the corresponding $M-\theta_r$ curves.

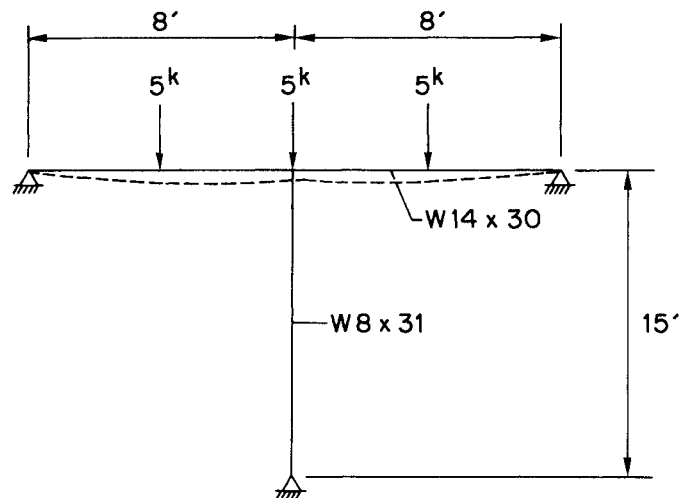
In addition to column shortening, there is bending deformation in the column. As a result of bending, the joint will rotate. If rotation is in the direction as shown in Fig. 21a, the direction of moment induced will be that as shown in Fig. 21d. The induced moment to the left of the joint has the same direction as that of Fig. 21b but the direction of the induced moment to the right of the joint has opposite direction to that of Fig. 21b. In other words, the connection to the left of the columns will load while the connection to the right of the column will unload as a result of joint rotation.

Since the two column deformations, shortening and bending, occur simultaneously as P applies, the phenomenon depicted in Figs. 21c and 21d are concurrent events. Consequently, the connection on the left-hand side of the column may follow path $A'B'$ or $A'C'$ (i.e. unload or load) depending on whether M_{2L} is greater or smaller than M_{3L} . On the other hand, the connection on the right-hand side of the column will always unload and so it will always exhibit a restraining effect to the column.

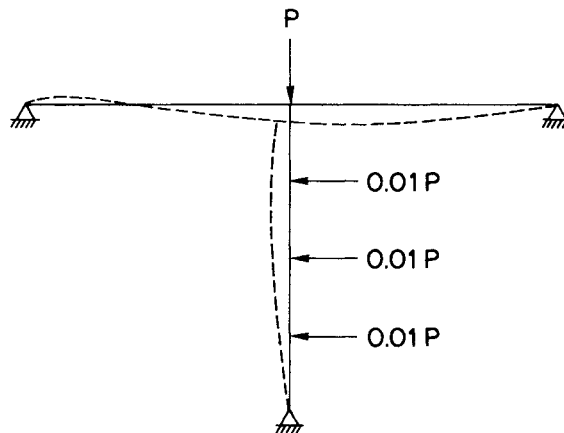
To study the behavior of flexibly connected frames, recourse to numerical methods is inevitable because of the inherent nonlinear nature of the problem. To give the reader an insight into the restraint characteristic between members of flexibly-connected frames, the behavior of the following subassembly will be discussed.

To study the behavior of flexibly connected frames, the subassemblies shown in Figs. 22 and 23 are analyzed with the two load sequences applied as shown. The difference between the subassembly of Fig. 22 and Fig. 23 is that rigid connections are assumed in the subassembly of Fig. 22 and flexible connections with a moment-rotation behavior of Fig. 24 are used in the subassembly of Fig. 23. The loadings for the two subassemblies are identical. The two beams are first loaded at midspan with a 5-kip concentrated load in load sequence 1. The column is also loaded with a 5-kip concentrated load in load sequence 1. The column loads (vertical at the joint and horizontal at quarter-points of the columns) are then applied monotonically in load sequence 2 until a plastic hinge formed in the column.

The distribution of joint moments for the rigidly connected and flexibly connected subassemblies are shown



(a) Load Sequence 1



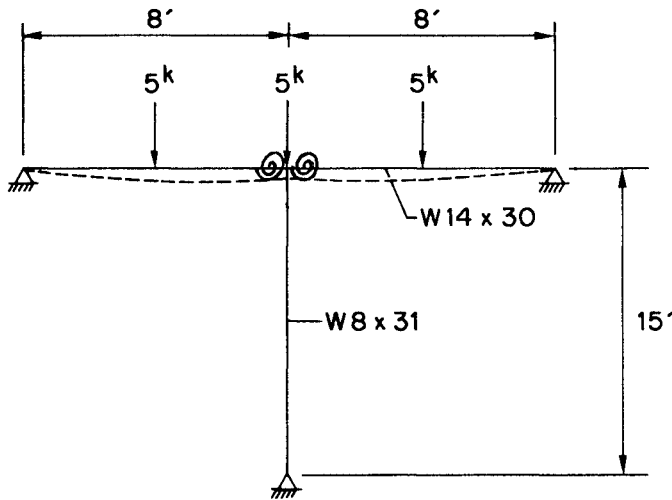
(b) Load Sequence 2

Fig. 22. Rigidly connected T-shaped subassembly

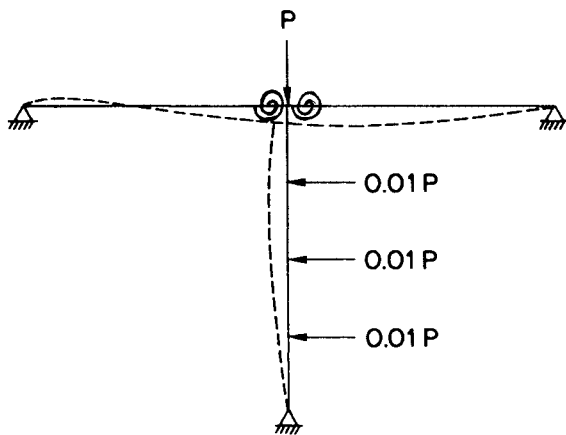
in Figs. 25a and b respectively. The following observations can be made from the plots:

1. The column is restrained against buckling even though the beams are preloaded. For the rigidly connected subassembly, restraint is offered by the left beam until at $P = 38$ kips the right beam starts to provide the restraint. At $P = 54$ kips, restraint is offered solely by the right beam. For the flexibly connected subassembly both beams provide the restraint to the column.
2. The restraining effect is more pronounced for rigid connections than for flexible connections.

The difference in moment distribution around the joint



(a) Load Sequence 1



(b) Load Sequence 2

Fig. 23. Flexibly connected T-shaped subassembly

is apparent in Fig. 25. Of particular interest is the direction of M_{BL} . For the flexibly connected subassembly, M_{BL} is always negative whereas for the rigidly connected subassembly M_{BL} is only negative at low values of P but becomes positive at high values of P . The reason for this can be explained by reference to Fig. 26 in which the beam end moments at the joint are decomposed. At the end of load Sequence 1, M_{BL} is negative (i.e. counterclockwise, Fig. 26a). However, as load sequence 2 commences, the induced moment M_{BL} may be positive (i.e. clockwise, Fig. 26b) as a result of joint translation or negative (i.e. counterclockwise, Fig. 26c) as a result of joint rotation. Whether the final value of M_{BL} is positive or negative depends on whether joint translation or joint rotation dominates.

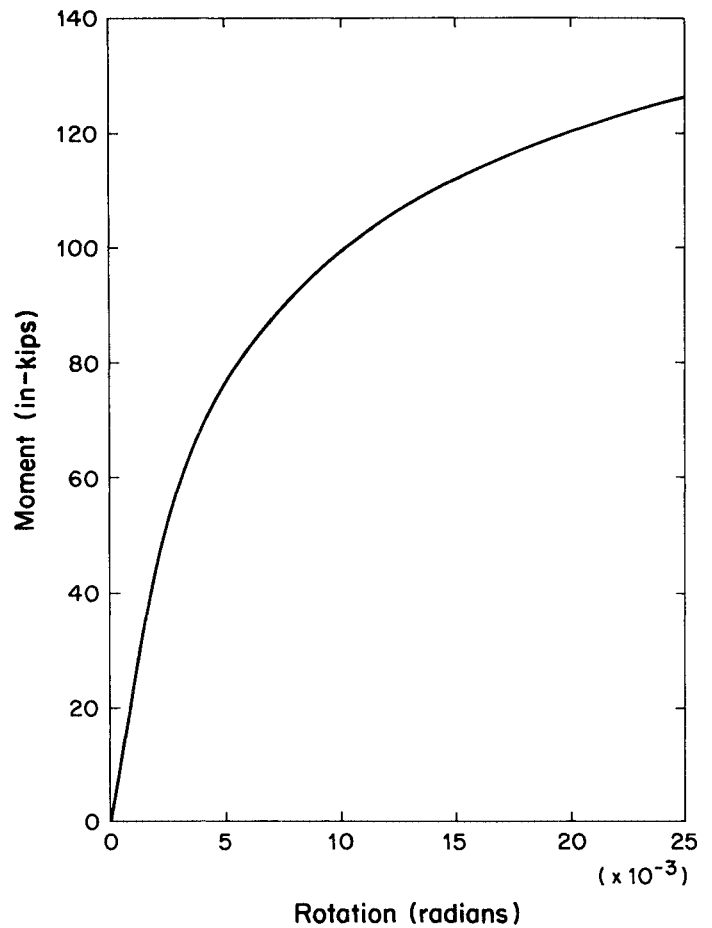


Fig. 24. Connection moment-rotation behavior used for the T-shaped subassembly

In Fig. 27, the magnitude of joint translation and joint rotation as a function of the applied force P are plotted. Although the magnitude of joint translation for both the rigidly connected and flexibly connected subassemblies are comparable, the joint rotation of the flexibly connected subassembly is significantly larger than that of the rigidly connected subassembly. As a result, the moment induced as a result of joint rotation will outweigh that of joint translation, hence the final value of M_{BL} for the flexibly connected frame is negative.

As for the right beam, regardless of whether joint translation or joint rotation dominates, the induced M_{BR} is almost always negative. As a result, this beam, except at the initial loading stage for the rigidly connected subassembly, will always provide restraint to the column regardless of whether the connection is rigid or flexible. It should be mentioned that unloading occurs at the connection which connects the right beam to the column as load sequence 2 commences because the direction of moment at this location is opposite for load sequence 1

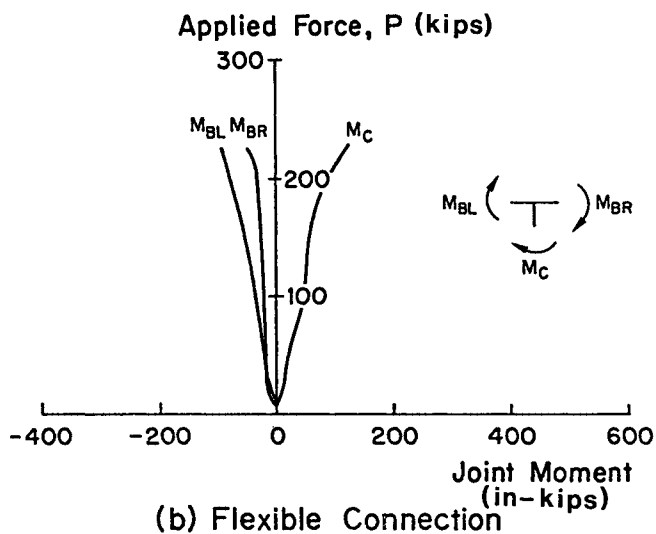
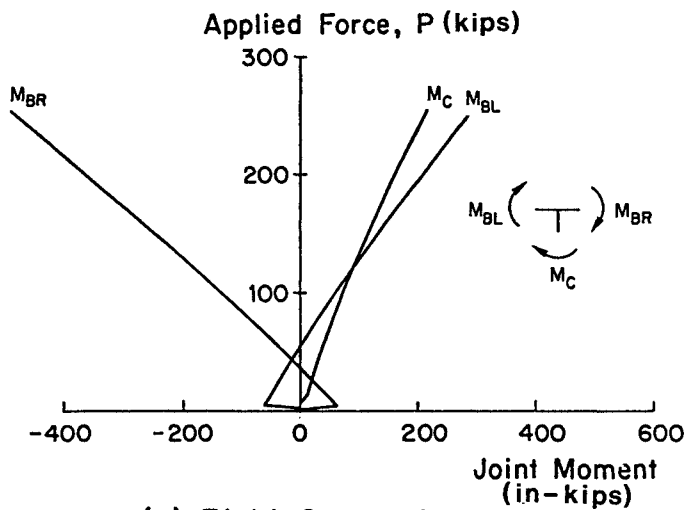
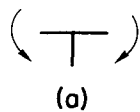
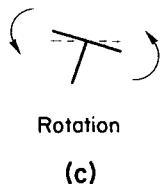
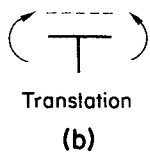


Fig. 25. Applied force vs. joint moment relationships



Joint moment at the end of load sequence 1



Joint moment induced as a result of load sequence 2

Fig. 26. Decomposition of joint moments

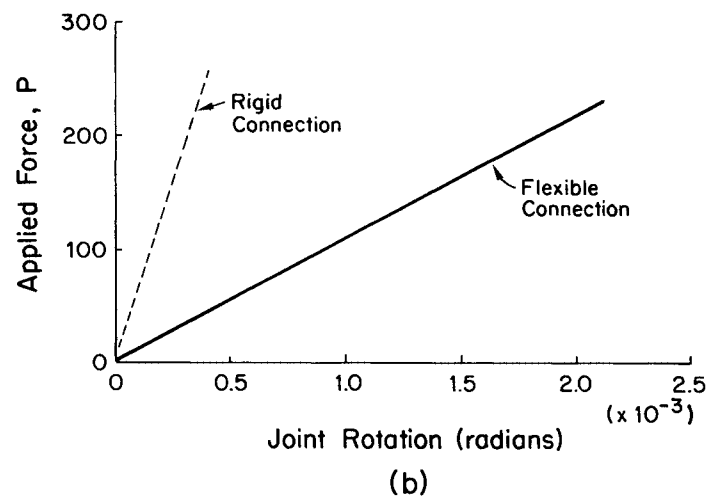
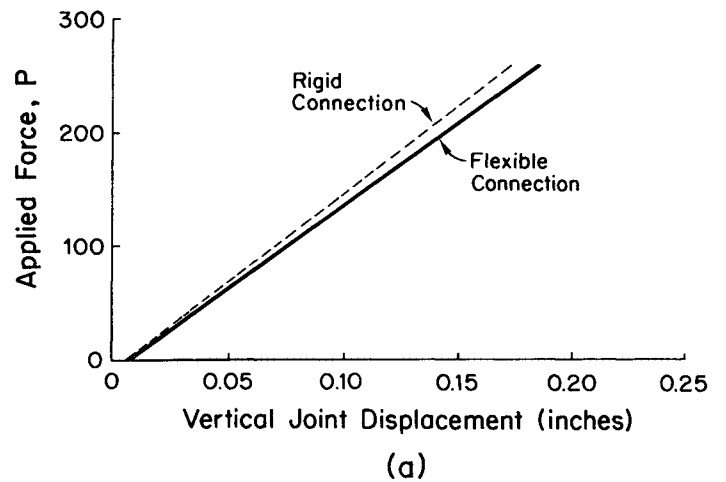


Fig. 27. Joint displacement and rotation of the T-shaped subassembly

and load sequence 2 (see Fig. 26). Consequently, the left connection is offering tangent stiffness restraint to the column whereas the right connection is offering initial stiffness restraint.

A more detailed analysis and discussion of the behavior of subassemblies with flexible connections are given elsewhere.³⁸

7. DESIGN OF COLUMNS WITH SEMI-RIGID CONNECTIONS

For design purposes, if the connections are rigid, one can just perform a first-order analysis on a trial frame. With the end moments and axial force known for each member, an interaction formula (to be discussed in the next section) can be used to check the trial sizes of the members. However, if the connections are not rigid, then care must be exercised in using the interaction equations in the proposed LRFD Specifications,¹³ because the

maximum moment in the member as determined by Eq. 32 will not be valid anymore, since the moment amplification factors B_1 and B_2 are only defined for rigidly connected frames.

One plausible solution is to use computer-aided analysis and design in which a second-order analysis is performed on the flexibly connected frame to determine the maximum moment including the P - δ and P - Δ effects directly. However, in lieu of such analysis, simplified design methods based on idealized connection behavior have been proposed.^{21,38,41,42}

Additional Studies

Additional studies on the role of connections in effecting the strength and stiffness of frames have been reported by Ackroyd,⁴³ Moncarz and Gerstle⁴⁴ and Simitzes et al.^{45,46,47} In Ref. 43, it was shown an increase in connection stiffness does not always result in an increase in frame strength. For long-span frames only a few stories high where the lateral loads effects are small compared with gravity loads, an increase in connection stiffness may cause a decrease in frame strength. A parameter was defined which can be used as an index to determine whether providing over stiff connections will be beneficial or detrimental.

In addition to connection flexibility, another important factor that affects the limit state behavior of a frame is panel zone deformation. The study of panel zone deformation on frame behavior has been reported by Fielding et al.,^{48,49} Becker,⁵⁰ Kato⁵¹ and Krawinkler.⁵² In these studies, attention was given to the modeling of the shear deformation of the panel zone. The important results of these studies were summarized by the authors.⁵³ Recently, a finite element model of the panel zone which can represent all modes (extension, shear, bending) of deformation of the panel zone has been reported.³⁸ Generally speaking, the strength and stiffness of frames will be reduced if the effect of panel zone deformation is taken into account in the analysis procedures.

It should be mentioned that since both connection flexibility and panel zone deformation have detrimental effects on frame strength and stiffness, particular attention must be given by the designers to ensure that the strength of the frame is adequate and that the stability and drift will not be a problem for Type PR frames.

8. BEAM-COLUMN INTERACTION FORMULAS

With the end moments and axial force of a member known, the member can be proportioned so that it can resist these applied forces without premature failure. For design purposes, the proportion of the member is facilitated by the use of interaction formulas. The general form of an interaction formula is

$$f\left(\frac{P_u}{P_n}, \frac{M_{ux}}{M_{nx}}, \frac{M_{uy}}{M_{ny}}\right) \leq 1.0 \quad (40)$$

where P_u , M_{ux} , M_{uy} are the design axial load and bending moments (required strength) about the principal axes respectively and P_n , M_{nx} and M_{ny} are the corresponding ultimate axial force and moment capacities of the section. Interaction equations can be linear or nonlinear. A linear interaction equation is an equation in which the terms P_u/P_n , M_{ux}/M_{nx} , M_{uy}/M_{ny} are combined together linearly. A nonlinear interaction equation is one in which these terms are combined together nonlinearly.

Linear Interaction Equations

The AISC/LRFD Specification, based on the exact inelastic solution of 82 beam-columns,⁵⁴ proposed the following interaction equations for sway and nonsway beam-columns

$$\text{for } \frac{P_u}{\phi_c P_n} \geq 0.2$$

$$\frac{P_u}{\phi_c P_n} + \frac{8}{9} \left(\frac{M_{ux}}{\phi_b M_{nx}} + \frac{M_{uy}}{\phi_b M_{ny}} \right) \leq 1.0 \quad (41)$$

$$\text{for } \frac{P_u}{\phi_c P_n} < 0.2$$

$$\frac{P_u}{2\phi_c P_n} + \frac{M_{ux}}{\phi_b M_{nx}} + \frac{M_{uy}}{\phi_b M_{ny}} \leq 1.0 \quad (42)$$

The above interaction formulas are a simplification and clarification of interaction Formulas 1.6.1a and 1.6.1b used in the present AISC/ASD Specification.¹⁹ Equation 1.6.1a is a check for stability and Eq. 1.6.1b is a check for strength. Since the amplification factor B_1 can be less than unity in the AISC/ASD Specification, both equations are required to be checked in the design. However, in the AISC/LRFD Specification, since the B_1 factor must be greater than unity, only one equation needs to be checked. The applicable equation is governed by the value $P_u/\phi_c P_n$, where P_u is the axial force in the member, P_n is the axial strength capacity of the member and ϕ_c is the column resistance factor and has a value of 0.85.

M_{ux} and M_{uy} are the maximum moment (including the P - δ and P - Δ effects) in the member which may be determined from a second-order elastic analysis. However, in lieu of such analysis, their values may be determined from the simplified approach described in the section on Columns in Frames.

Nonlinear Interaction Equations

Equations 41 and 42 are applicable to members in both braced and unbraced frames. For members in braced frames, the new specification also recommended a non-

linear interaction equation based on the work in Ref. 55 for the design of I and wide-flange shapes. The equation has the form

$$\left(\frac{M_{ux}}{\phi_b M'_{px}}\right)^\xi + \left(\frac{M_{uy}}{\phi_b M'_{py}}\right)^\xi \leq 1.0 \quad (43)$$

$$\left(\frac{C_{mx} M_{ux}}{\phi_b M'_{nx}}\right)^\eta + \left(\frac{C_{my} M_{uy}}{\phi_b M'_{ny}}\right)^\eta \leq 1.0 \quad (44)$$

where

$$\xi = 1.6 - \frac{P_u P_y}{2[\ln(P_u P_y)]} \text{ for } 0.5 \leq b_f/d \leq 1.0 \quad (45)$$

$$\eta = \begin{cases} 0.4 + \frac{P_u}{P_y} + \frac{b_f}{d} \geq 1.0 & \text{for } b_f/d \geq 0.3 \\ 1 & \text{for } b_f/d < 0.3 \end{cases} \quad (46)$$

b_f = flange width, in.

d = member depth, in.

$$M'_{px} = 1.2 M_{px} [1 - (P_u/P_y)] \leq M_{px} \quad (47)$$

$$M'_{py} = 1.2 M_{py} [1 - (P_u/P_y)] \leq M_{py} \quad (48)$$

$$M'_{nx} = M_{nx} [1 - (P_u/\phi_c P_n)][1 - (P_u/P_{ex})] \quad (49)$$

$$M'_{ny} = M_{ny} [1 - (P_u/\phi_c P_n)][1 - (P_u/P_{ey})] \quad (50)$$

Design Evaluation

At this point, it is of interest to compare design carried out using the ASD format and the new LRFD format. A comprehensive comparative study was reported by Zhou and Chen.⁵⁶ In the study, a number of nonsway beam-columns under a specific set of force conditions were designed using both the ASD and LRFD formats. For the LRFD format, both the linear (LRFD-Linear) and nonlinear (LRFD-Non) interaction equations were used. The result of the comparison was expressed by the weight ratios of the sections chosen using the various design formats and interaction equations.

Figure 28 shows one such comparison. It can be seen that for single curvature bending ($C_{mx} = C_{my} = 1$), the LRFD approach is generally more liberal than the ASD approach. Figure 29 shows the distributions of the weight ratios for the beam-columns designed using live load to dead load (L_n/D_n) ratios of 1, 3 and 5 respectively. A constant roof live load to dead load (L_r/D_n) ratio of 0.2 was used for all three cases. From the figure, it can be seen that

1. The smaller the L_n/D_n ratio is, the more liberal is the LRFD approach as compared to the ASD approach.
2. The LRFD nonlinear equations will give the lightest section (except in cases when b_f/d ratio is small and the ratio of moment to axial force is large when the

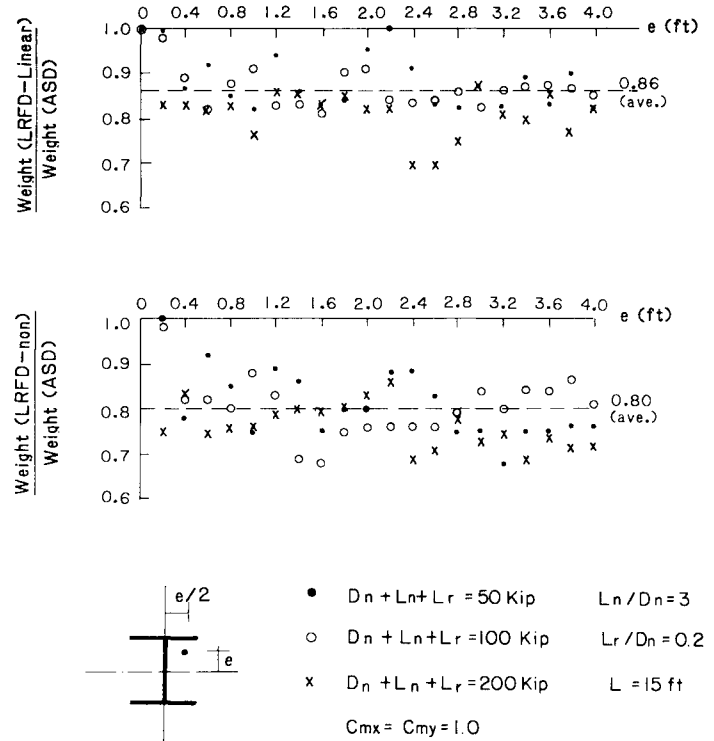


Fig. 28. Weight ratio

LRFD linear equations give a more economical section).

The readers are referred to Ref. 56 for a more thorough discussion of the comparison.

Nonlinear Interaction Equations for Box Columns

Before leaving the subject, it is necessary to discuss recent development of the interaction equations for rectangular box beam-columns under biaxial loading. Based on a study by Zhou and Chen,⁵⁷ the following interactions are proposed as an extension of the expressions proposed previously by Chen and McGraw⁵⁸ for welded square box columns under biaxial loading to the present more general case of rectangular box cross section.

For short members

$$\left(\frac{M_{ux}}{M'_{px}}\right)^\xi + \left(\frac{M_{uy}}{M'_{py}}\right)^\xi \leq 1.0 \quad (51)$$

where

$$\xi = 1.7 - \frac{P_u P_y}{\ln(P_u P_y)} \quad (52)$$

$$M'_{px} = 1.2 (1 - P_u/P_y) M_{px} \leq M_{px} \quad (53)$$

$$M'_{py} = 1.2 (1 - P_u/P_y) M_{py} \leq M_{py} \quad (54)$$

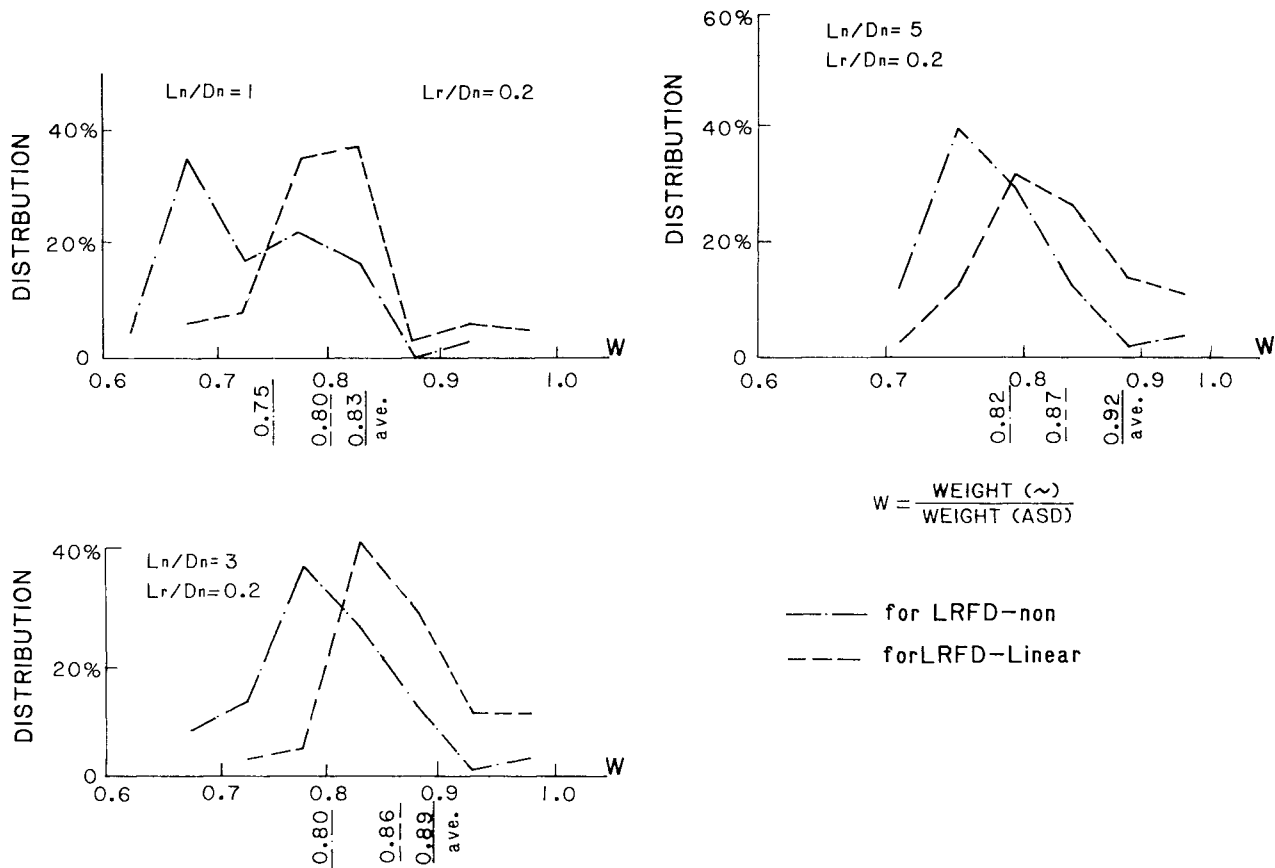


Fig. 29. Distribution of weight ratio

For long members

$$\left(\frac{M_{ux}}{M'_{nx}}\right)^\alpha + \left(\frac{M_{uy}}{M'_{ny}}\right)^\alpha \leq 1.0 \quad (55)$$

where

$$\alpha = 1.7 - \frac{P_u/P_y}{\ln(P_u/P_y)} - a \frac{KL}{r} (P_u/P_y)^b \geq 1.1$$

$$M'_{nx} = M_{nx} (1 - P_u/P_n) \left[1 - \frac{P_u}{P_{ex}} \frac{1.25}{(B/H)^{1/3}} \right] \quad (56)$$

$$M'_{ny} = M_{py} (1 - P_u/P_n) \left[1 - \frac{P_u}{P_{ex}} \frac{1.25}{(B/H)^{1/2}} \right]$$

in which

B = width and H = depth of the cross section

$$a = \begin{cases} 0.06 & \text{if } P_u/P_y \leq 0.4 \\ 0.15 & \text{if } P_u/P_y > 0.4 \end{cases} \quad (57)$$

$$b = \begin{cases} 1.0 & \text{if } P_u/P_y \leq 0.4 \\ 2.0 & \text{if } P_u/P_y > 0.4 \end{cases} \quad (58)$$

These nonlinear interaction formulas have been shown⁵⁷ to compare favorably with computer solutions and some experimental results.

9. SUMMARY AND CONCLUSIONS

In this paper, the state-of-the-art design philosophies with particular emphasis on the Load and Resistance Factor Design (LRFD) format are discussed. The background and relevant development of the design methods relating to columns and beam-columns are presented.

LRFD is a limit-state design method. A valid limit-state analysis and design of structures or structural members requires more understanding of structural behavior and more demand on structural analysis techniques. For example, in the AISC/LRFD Specification, a direct second-order analysis of the structure to determine the maximum design forces in the member is recommended. Furthermore, an extensive use of stability theory is employed in the development of the specification equations.

Although first-order theory is still extensively used by engineers and designers in proportioning members, the use of second-order analysis will become more and more popular in the near future. The use of more sophisticated analysis techniques is enhanced by the rapid development in computer hardware and software. In particular, the great advancement in microcomputers has enabled engineers and designers to perform fast and more effi-

cient analysis and design of most structural members. Consequently, computer-aided analysis and design of structure will continue to gain popularity as time proceeds.

In addition to theoretical investigations of structural behavior, the continued need for experimental investigations is inevitable, especially in the area of connection restraint characterization. Theoretical and experimental work must go in parallel paths to ensure the continued development of more economical and rational design procedures in view of recent great advancement in microcomputers.

REFERENCES

1. Euler, L. De Curvis Elasticis *Lausanne and Geneva 1744*, pp. 267–268. The Euler formula was derived in a later paper, *Sur le Forces des Colonnes Memoires de l'Academie Royale des Sciences et Belles Lettres*, Vol. 13, Berlin, 1759.
2. Engesser, F. Zeitschrift fur Architektur und Ingenieurwesen 35, 1889, p. 455. *Schweizerische Bauzeitung* Vol. 26, 1895, p. 24.
3. Considere, A. Resistance des Pieces Comprimees *Congres International des Procedes de Construction Paris*, Vol. 3, 1891, p. 371.
4. Shanley, F. R. Inelastic Column Theory *Journal of the Aeronautical Sciences*, Vol. 14, No. 5, May 1947, pp. 261–264.
5. Duberg, J. E. and T. W. Wilder Column Behavior in the Plastic Stress Range *Journal of the Aeronautic Science*, Vol. 17, No. 6, 1950.
6. Johnston, B. G. Buckling Behavior Above the Tangent Modulus Load *Journal of the Engineering Mechanics Division, ASCE*, Vol. 87, No. EM6, December 1961, pp. 79–99.
7. Johnston, B. G. Column Buckling Theory: Historic Highlights *ASCE, Journal of Structural Engineering*, Vol. 109, No. 9, September 1983, pp. 2086–2096.
8. Timoshenko, S. P. and J. M. Gere Theory of Elastic Stability 2nd Ed., *Engineering Societies Monographs, McGraw-Hill, New York, N.Y.*, 1961.
9. Bleich, F. Buckling Strength of Metal Structures *Engineering Societies Monographs, McGraw-Hill, New York, N.Y.*, 1952.
10. Chen, W. F. and T. Atsuta Theory of Beam-Columns: Vol. 1—In-plane Behavior and Design *McGraw-Hill, New York, N.Y.*, 1976.
11. Chen, W. F. and T. Atsuta Theory of Beam-Columns: Vol. 2—Space Behavior and Design *McGraw-Hill, New York, N.Y.*, 1977.
12. Lui, E. M. and W. F. Chen End Restraint and Column Design Using LRFD *AISC Engineering Journal*, Vol. 20, No. 1, 1st Qtr., 1983, pp. 29–39.
13. American Institute of Steel Construction, Inc. Proposed Load and Resistance Factor Design Specification for Structural Steel Buildings *Chicago, Ill.*, January 1985.
14. Johnston, B. G., Ed. Guide to Design Criteria for Metal Compression Members *Column Research Council*, 1960.
15. Bjorhovde, R. Deterministic and Probabilistic Approaches to the Strength of Steel Columns *Ph.D. Dissertation, Department of Civil Engineering, Lehigh University, Bethlehem, Pa.*, 1972.
16. Johnston, B. G., Ed. SSRC Guide to Stability Design Criteria for Metal Structures 3rd Ed., *John Wiley, New York, N.Y.*, 1976.
17. Rondal, J. and R. Maquoi Single Equation for SSRC Column Strength Curves *Technical Notes ASCE Journal of the Structural Division*, Vol. 105, No. ST1, New York, N.Y., January 1979, pp. 247–250.
18. Lui, E. M. and W. F. Chen Simplified Approach to the Analysis and Design of Columns with Imperfections *AISC Engineering Journal*, Vol. 21, No. 2, 2nd Qtr., 1984.
19. American Institute of Steel Construction, Inc. Specification for the Design, Fabrication and Erection of Structural Steel for Buildings *Chicago, Ill.*, November, 1978.
20. Lui, E. M. and W. F. Chen Strength of H-Columns with Small End Restraints *The Journal of the Institute of Structural Engineers*, Vol. 61B, No. 1, London, March 1983, pp. 17–26.
21. Bjorhovde, R. Effect of End Restraint on Column Strength—Practical Applications *AISC Engineering Journal*, Vol. 21, No. 1, 1st Qtr., 1984, pp. 1–13.
22. Lui, E. M. and W. F. Chen Discussion on Effect of End Restraint on Column Strength—Practical Applications by R. Bjorhovde to appear, 1985.
23. Iwankiw, N. Note on Beam-Column Moment Amplification Factor *AISC Engineering Journal*, Vol. 21, No. 1, 1st Qtr., 1984, pp. 21–23.
24. Austin, W. J. Strength and Design of Metal Beam-Columns *ASCE Journal of Structural Division*, Vol. 87, No. ST4, April 1961, pp. 1–32.
25. Massonnet, C. Stability Considerations in the Design of Steel Columns *ASCE Journal of Structural Division*, Vol. 85, No. ST7, September 1959, pp. 75–111.
26. Rosenblueth, E. Slenderness Effects in Buildings *ASCE Journal of the Structural Division*, Vol. 91, No. ST1, February 1965, pp. 229–252.
27. Stevens, L. K. Elastic Stability of Practical Multi-story Frames *Proceedings, Institute of Civil Engineers*, Vol. 36, London, England, 1967.
28. Cheong-Siat-Moy, F. Consideration of Secondary Effects in Frame Design *ASCE Journal of Structural Division*, Vol. 103, No. ST10, October 1972, pp. 2,005–2,019.
29. Yura, J. A. The Effective Length of Columns in Unbraced Frames *AISC Engineering Journal*, Vol. 8, No. 2, April 1971, pp. 37–42.
30. McGuire, W. Geometrical Nonlinear Analysis and Amplification Factors *Private Communication, August 1984*.

31. *LeMessurier, W. J.* A Practical Method of Second-Order Analysis, Part 2—Rigid Frames *AISC Engineering Journal*, Vol. 14, No. 2, 2nd Qtr., 1972, pp. 49–67.
32. *Rathbun, J. C.* Elastic Properties of Riveted Connections *Transactions of the American Society of Civil Engineers*, Vol. 101, 1936, pp. 524–563.
33. *Romstad, K. M. and C. V. Subramanian* Analysis of Frames with Partial Connection Rigidity *ASCE Journal of the Structural Division*, Vol. 96, No. ST11, November, 1970, pp. 2,283–2,300.
34. *Razzaq, Z.* End Restraint Effect on Steel Column Strength *ASCE Journal of the Structural Division*, Vol. 109, No. ST2, February 1983, pp. 314–334.
35. *Frye, M. J. and G. A. Morris* Analysis of Flexibly Connected Steel Frames *Canadian Journal of Civil Engineers*, Vol. 2, No. 3, Canada, September 1975, pp. 280–291.
36. *Jones, S. W., P. A. Kirby and D. A. Nethercot* Columns with Semirigid Joints *ASCE Journal of the Structural Division*, Vol. 108, No. ST2, February 1982, pp. 361–372.
37. *Colson, A. and J. M. Louveau* Connections Incidence on the Inelastic Behavior of Steel Structures *Euromech Colloquium 174*, October 1983.
38. *Lui, E. M.* Effects of Connection Flexibility and Panel Zone Deformation on the Behavior of Plane Steel Frames *Ph.D. Dissertation, Department of Structural Engineering, School of Civil Engineering, Purdue University, West Lafayette, Ind., 1985.*
39. *Lewitt, C. S., E. Chesson and W. H. Munse* Restraint Characteristics of Flexible Riveted and Bolted Beam-To-Column Connections *Engineering Experiment Station Bulletin No. 500, University of Illinois at Urbana-Champaign, Ill., January 1969.*
40. *Sugimoto, H.* Study of Offshore Structural Members and Frames *Ph.D. Dissertation, Department of Structural Engineering, School of Civil Engineering, Purdue University, West Lafayette, Ind., 1983.*
41. *Disque, R. O.* Directional Moment Connections—A Proposed Design Method for Unbraced Steel Frames *AISC Engineering Journal*, 1st Qtr., 1975, pp. 14–18.
42. *Driscoll, G. C.* Effective Length of Columns with Semi-Rigid Connections *AISC Engineering Journal*, 4th Qtr., 1976, pp. 109–115.
43. *Ackroyd, M. H.* Nonlinear Inelastic Stability of Flexibly-Connected Plane Steel Frames *Ph.D. Dissertation, Department of Civil, Environmental and Architectural Engineering, University of Colorado, Boulder, Colo., 1979.*
44. *Moncarz, P. D. and K. H. Gerstle* Steel Frames with Non-Linear Connections *ASCE Journal of the Structural Division*, Vol. 107, No. ST8, August, 1981, pp. 1,427–1,441.
45. *Simitses, G. J. and A. S. Vlahinos* Stability Analysis of a Semi-Rigidly Connected Simple Frame *Journal of Constructional Steel Research*, Vol. 2, No. 3, September 1982, pp. 29–32.
46. *Simitses, G. J. and J. Giri* Non-Linear Analysis of Unbraced Frames of Variable Geometry *International Journal of Non-Linear Mechanics*, Vol. 17, No. 1, 1982, pp. 47–61.
47. *Simitses, G. J., J. D. Swisshelm and A. S. Vlahinos* Flexibly-Jointed Unbraced Portal Frames *Journal of Constructional Steel Research*, Vol. 4, 1984, pp. 27–44.
48. *Fielding, D. J. and J. S. Huang* Shear in Beam-To-Column Connections *The Welding Journal*, Vol. 50, July 1971.
49. *Fielding, D. J. and W. F. Chen* Frame Analysis and Connection Shear Deformation *ASCE Journal of the Structural Division*, Vol. 99, No. ST1, January 1973, pp. 1–18.
50. *Becker, R.* Panel Zone Effect on the Strength and Stiffness of Steel Rigid Frames *AISC Engineering Journal*, Vol. 12, No. 1, 1st Qtr., 1975, pp. 19–29.
51. *Kato, B.* Beam-To-Column Connection Research in Japan *ASCE Journal of the Structural Division*, Vol. 108, No. ST2, February 1982, pp. 343–360.
52. *Krawinkler, H.* Shear in Beam-Column Joints in Seismic Design of Steel Frames *AISC Engineering Journal*, 3rd Qtr., 1978, pp. 82–91.
53. *Chen, W. F. and E. M. Lui* Effects of Connection Flexibility and Panel Zone Shear Deformation on the Behavior of Steel Frames Seminar on Tall Structures and Use of Prestressed Concrete in Hydraulic Structures *Indian National Group of the International Association for Bridge and Structural Engineering, Srinagar, May 24–26, 1984, pp. 155–176.*
54. *Kanchanalai, T.* The Design and Behavior of Beam-Columns in Unbraced Steel Frames *AISI Project No. 189, Report No. 2, Civil Engineering/Structures Research Lab, University of Texas at Austin, October 1977.*
55. *Tebedge, N. and W. F. Chen* Design Criteria for H-Columns Under Biaxial Bending *ASCE Journal of the Structural Division*, Vol. 104, No. ST9, September 1978, pp. 1,355–1,370.
56. *Zhou, S. P. and W. F. Chen* A Comparative Study of Beam-Columns in ASD and LRFD *Structural Engineering Report No. CE-STR-84-53, School of Civil Engineering, Purdue University, West Lafayette, Ind., 1984.*
57. *Zhou, S. P. and W. F. Chen* Design Criteria for Box Beam-Columns Under Biaxial Loading *Structural Engineering Report No. CE-STR-85-2, School of Civil Engineering, Purdue University, West Lafayette, Ind., 1985.*
58. *Chen, W. F. and J. McGraw* Behavior and Design of HSS-Columns Under Biaxial Bending *Proceedings of 2nd Engineering Mechanics Division Specialty Conference, Raleigh, N.C., May 23–25, 1977.*